

Article

Optimizing the Timeliness of Hybrid OFDMA-NOMA Sensor Networks with Stability Constraints

Wei Wang¹, Yunquan Dong^{1,2}  and Chengsheng Pan^{1,*}

¹ School of Electronic and Information Engineering, Nanjing University of Information Science and Technology, Nanjing 210044, China; 20211218024@nuist.edu.cn (W.W.); yunquandong@nuist.edu.cn (Y.D.)

² School of Electronic and Information Engineering, Anhui Jianzhu University, Hefei 230601, China

* Correspondence: 003150@nuist.edu.cn

Abstract: In this paper, we analyze the timeliness of a multi-user system in terms of the age of information (AoI) and the corresponding stability region in which the packet rates of users lead to finite queue lengths. Specifically, we consider a hybrid OFDMA-NOMA system where the users are partitioned into several groups. While users in each group share the same resource block using non-orthogonal multiple access (NOMA), different groups access the fading channel using orthogonal frequency division multiple access (OFDMA). For this system, we consider three decoding schemes at the service terminals: interfering decoding, which treats signals from other users as interference; serial interference cancellation, which removes signals from other users once they have been decoded; and the enhanced SIC strategy, where the receiver attempts to decode for another user if decoding for a previous user fails. We present the average AoI for each of the three decoding schemes in closed form. Under the constraint of the stable region, we find the minimum AoI of each decoding scheme efficiently. The numerical results show that by optionally choosing the decoding scheme and transmission rate, the hybrid OFDMA-NOMA outperforms conventional OFDMA in terms of both system timeliness and stability.

Keywords: age of information; orthogonal frequency division multiple access; non-orthogonal multiple access; stability; timeliness



check for updates

Citation: Wang, W.; Dong, Y.; Pan, C. Optimizing the Timeliness of Hybrid OFDMA-NOMA Sensor Networks with Stability Constraints. *Electronics* **2024**, *13*, 1768. <https://doi.org/10.3390/electronics13091768>

Academic Editor: Christos J. Bouras

Received: 11 April 2024

Revised: 29 April 2024

Accepted: 1 May 2024

Published: 3 May 2024



Copyright: © 2024 by the authors. Licensee MDPI, Basel, Switzerland. This article is an open access article distributed under the terms and conditions of the Creative Commons Attribution (CC BY) license (<https://creativecommons.org/licenses/by/4.0/>).

1. Introduction

In recent years, the development of 5G/6G and next-generation wireless communication has led to the emergence of the Internet of Things (IoT) [1]. As the IoT's supporting technology, wireless sensor networks are widely deployed in a variety of real-time monitoring applications [2]. However, transmitting time-sensitive information wirelessly requires strict standards for stability and timeliness.

Stability and timeliness are two crucial metrics in wireless sensor networks. Traditional metrics, such as latency and throughput, which describe end-to-end delay and data processing capabilities [3], may not be effective for applications with strict timeliness requirements. These metrics cannot fully capture the issue of reduced timeliness caused by sudden information updates. To this end, Kaul et al. proposed AoI as a new metric for measuring the freshness of information [4]. AoI indicates the freshness of the latest received information accurately, particularly for time-sensitive information. Stability is a crucial metric for assessing transmission performance and ensuring the timeliness of a network. The transmission of information from traditional monitoring equipment is stable when using wired cables. This method has the advantage of being less susceptible to interference from transmission scenarios and other signals. However, the complexity of wiring increases both time and maintenance costs [5]. Wireless transmission monitoring equipment is not bound by the data line flexibility of independent deployment. It is easy to deploy and has faster maintenance compared to independent deployment, but it is highly susceptible to interference from signals of the same frequency [6].

If the focus is solely on the stability of the transmission process, it may lead to smaller transmission latency. However, waiting for and retransmitting data may also reduce the timeliness of received information. Excessive pursuit of timeliness may render the transmission process unstable in the actual system due to inter-user interference. Therefore, there is an urgent need to improve both the stability and timeliness of the wireless transmission process.

Network access mechanisms are crucial for wireless communication. One such mechanism is OFDMA technology [7], which allocates multiple mutually orthogonal subcarriers to multiple users for simultaneous transmission. In OFDMA, each user is assigned an independent resource block, ensuring dedicated transmission channels. NOMA, on the other hand, shares the spectrum by allocating an entire resource block to multiple users simultaneously [8]. It relies on successive interference cancellation (SIC) to decode signals from the overlapping transmissions [9]. By integrating the strengths of both OFDMA and NOMA, the stability and timeliness of information transmission in research can be significantly enhanced.

In this paper, we consider the issues of stability and timeliness in wireless sensor networks with hybrid OFDMA-NOMA access mechanisms.

1.1. Motivations

Since both stability and timeliness are important, we are motivated to consider the following issues:

How can we design a transmission mechanism that not only guarantees stability up to a defined threshold but also concurrently enhances timeliness?

Since Shannon's foundational 1948 paper on information theory [10], most research studies have focused on the saturated traffic model, where infinite amounts of stored data need to be transmitted. However, this approach ignores the burstiness of traffic and the importance of information timeliness in communication.

In a practical communication network, a user may receive traffic in bursts, meaning that there are periods when the transmission queue is empty [11]. Burst-arriving traffic refers to the random arrival of data, which can result in received packets becoming stale and unusable before the next update packet arrives. Thus, AoI has emerged as a new metric for measuring the freshness of information. AoI is the amount of time that passes between creating a packet that is successfully delivered and when the packet is received by the recipient. In contrast to traditional latency measures, AoI considers not just the frequency of packet updates but also transmission delays. AoI indicates the freshness of received information. The larger the AoI, the more stale the information. This metric is objective and accurately describes the age of received information. Therefore, using AoI as a metric for timeliness can effectively portray the system's performance in handling bursty traffic.

The notion of stable areas arose as a result of research into bursty network traffic. In such networks, users receive traffic in bursts, with data being queued in a buffer awaiting transmission. For system stability, it is important to prevent the queue from growing indefinitely. Stability analysis can be challenging due to the interaction between multiple queues [12], which can complicate the characterization of the service process. The following is an example of the OFDMA-NOMA system. In a hybrid OFDMA-NOMA system [13], users are organized into groups, with frequency resources allocated orthogonally to each group within the same time slot. This ensures efficient use of the available resources. Each group is assigned a resource block, and NOMA-based SIC technology provides services to the users within the group. Analyzing stability becomes more complex due to the interactive coupling of bursty traffic among users within a subgroup. Additionally, while the conventional SIC decoding scheme alleviates the decoding difficulty for post-sending users to some extent, it still has limitations. This limitation arises because a decoding failure for one user halts the decoding process for subsequent users. Therefore, it is necessary to consider multiple decoding methods to handle various transmission scenarios.

The system's stable transmission ensures timely information updates. However, stability alone does not guarantee that the system is up-to-date. When the sensor node generates packets at a lower frequency, the service terminal receives stale information, leading to an increase in AoI. Conversely, when the sensor node generates packets at a higher frequency, packets may not be serviced in a timely manner due to system performance limitations, causing them to accumulate in the queue. This also results in the service terminal observing stale information. It is important to maintain a stable transmission process to avoid this problem. Thus, achieving optimal timeliness depends on stability, but it still requires exploring specific optimization methods.

In this paper, we analyze the stability of the system in detail for the problem of multi-user bursty traffic in hybrid OFDMA-NOMA systems. To address user interactions, we explore various decoding methods that are suitable for different transmission scenarios. Building upon the system's stable transmission, we incorporate AoI as a metric to assess system timeliness. We designed a novel algorithm to optimize system timeliness without compromising stability.

1.2. Related Works

The stability of wireless information transmission has received significant attention in recent years. Jeon et al. analyzed the stable region of the transmission process from the primary source node and the secondary node to the destination node, assuming the capture effect [14]. They obtained the maximum stable throughput of the primary sensor node. Kompella et al. found that identifying stabilization regions in random access systems with three or more bursty sources presents a significant challenge [15]. This is due to interference created by each source when its transmission queue is not empty, which affects the others. In a queueing system, the service process of one queue is determined by the condition of the other queues, known as interacting queues [16,17]. Characterizing the stabilization region accurately presents a challenge due to the interactions between the cohorts. In [18], the authors investigate the maximum throughput of mobile radio-powered communication networks under mobile access points and the throughput maximization problem is divided into two layers (internal and external) to solve the maximization of the throughput of the WPCN under energy causality constraints. In [19], the authors address the energy supply problem of IoT nodes, a wireless-powered IoT is studied and a generated packet-based throughput maximization (GDPTM) algorithm is proposed to maximize the short-term throughput when the IoT nodes have enough energy to transmit the generated packets. In [20], the authors explore the trade-off between the achievable throughput of a sensor node and the energy harvesting opportunities, propose an energy thresholding approach, and prove the existence of an optimal energy threshold that maximizes the achievable throughput. In [21], the authors investigate the effect of perceived energy and data availability on the secondary throughput of an energy-harvesting cognitive radio network (EH-CRN). Research on stable transmission regions has primarily focused on throughput and delay, with only a few studies examining stable regions based on the AoI freshness measure. However, the stability boundary is crucial for ensuring timely system performance.

AoI has gained significant attention as a new metric for measuring timeliness in various communication environments. Theoretical studies of AoI focus on the number of source and destination nodes, service strategies, and queuing models. There are three analytical approaches to AoI: The first approach, proposed by Kaul et al., involves decomposing the area under the sawtooth function graph [22]. The second approach, by Yates et al., employs a stochastic hybrid system (SHS) [23]. This approach achieves variation in AoI through a simplified SHS model featuring a negative linear reset graph. The third approach, by Bedewy et al., utilizes an age penalty function to measure dissatisfaction with AoI [24].

The concept of AoI has been extended to applications in the context of IoT sensor networks. This extension has broadened theoretical research into AoI optimization within real-world scenarios. Optimizing AoI is a challenging task due to constraints such as

limited energy and the unavailability of updated data [25]. Kaul et al. analyzed the AoI in vehicular networks employing random access protocols for communication [4]. They showed that the solution to maximize throughput cannot be directly applied to minimize the AoI in random access channels. Zhang et al. conducted a study on edge caching systems, with a specific focus on mobile edge caching systems that take content updates into consideration [26]. They used AoI to measure content timeliness and proposed an optimized AoI-aware content update scheme. Mohammed et al. conducted a study on cognitive radio, focusing on the time division multiple access (TDMA) strategy, where only one user can transmit in a time slot, and the NOMA strategy, where multiple users can transmit in a single time slot [27]. The objective was to maximize throughput while adhering to the constraints of AoI. Maatouk et al. used the SHS approach to model the state update system, calculate the average AoI, and verify the performance benefits on a carrier sense multiple access (CSMA) system [28]. Li studied the timeliness of the CSMA/CA and slotted Aloha wireless networks, verifying the effect of arrival rate on AoI [3]. From the above studies, we found that there is a lack of studies applying AoI freshness measures to interaction cohorts.

Thus, we examine the interaction queue to ensure stable transmission in a hybrid OFDMA-NOMA system, utilizing the AoI metric.

1.3. Main Contributions

This paper investigates the impact of hybrid OFDMA-NOMA techniques on the uplink performance in the presence of random traffic. A discrete-time queuing model is applied to simulate the behavior of random traffic. We consider three decoding schemes: interference decoding (strategy A), serial interference cancellation (strategy B), and an enhanced SIC strategy with error handling (strategy C), while also addressing the drawbacks of existing SIC decoding schemes. The three schemes differ in how they treat signals from other users. Strategy A considers these signals as interference in all cases, while strategy B contrasts with strategy C. If strategy C fails to decode the first node, the second node can be decoded by considering the first node as interference. Employing the queuing model to simulate the communication process, we identify the stabilization region for an uplink hybrid OFDMA-NOMA system, incorporating all three decoding schemes. Additionally, we derive an exact functional expression for the average AoI of the system. We design a stabilizing iterative algorithm to rapidly determine the optimal AoI and arrival rate scheme tailored to the scenario at hand.

The contributions of this paper are summarized as follows.

- (1) In the hybrid OFDMA-NOMA system, we introduce three decoding schemes for service terminals, i.e., interference decoding, serial interference cancellation, and an enhanced SIC strategy with error handling. For each scheme, we derive the stable transmission region of the system, where each pair of data rates ensures the stability of the user queues.
- (2) We use AoI as a measure to evaluate the timeliness of these decoding schemes and derive an average AoI expression for each scheme. Furthermore, a stabilized iterative algorithm is introduced to ascertain the optimal AoI for the current transmission environment of the hybrid OFDMA-NOMA.
- (3) Our results show that in low signal-to-noise ratio (SNR) cases, interference decoding facilitates a reduced AoI while preserving transmission stability. In high SNR scenarios, an enhanced SIC strategy with error handling is more effective at minimizing the AoI and ensuring stable transmission.

1.4. Organization

The remainder of the paper is structured as follows: Section 2 describes the transmission model for wireless sensor networks, introducing definitions of queue stability and the AoI. Section 3 characterizes the stable transmission region for the three decoding schemes. The analysis and optimization of AoI, predicated on stability, are explored in Section 4.

Section 5 presents the experimental findings and examines the influence of various channel conditions on the network performance. Our concluding remarks are provided in Section 6.

2. System Model

We consider the real-time monitoring of a new energy vehicle battery. A total of $2G$ sensor nodes are responsible for independently monitoring the status information of the battery and transmitting the data to the service terminal in real time (and in a timely manner). In the uplink, we consider a hybrid OFDMA-NOMA system. The sensor nodes are divided into G groups, each based on OFDMA technology. This allows the frequency resources of the channel to be allocated orthogonally within the same time slot. There are a total of G subchannels, with one assigned to each group. Two sensor nodes in the group are served based on the NOMA technique. The system model is depicted in Figure 1. Given the analogous nature of the transmission processes observed in each group, we will proceed by examining group 1 as a representative example. In group 1, there are two sensor nodes, designated as B_i , where i ($i = 1, 2$) represents the i -th sensor node in the group. In the service process to group 1, both sensor nodes and service terminals rely on a single antenna to send or receive information. Time is split into time slots, indexed by n .

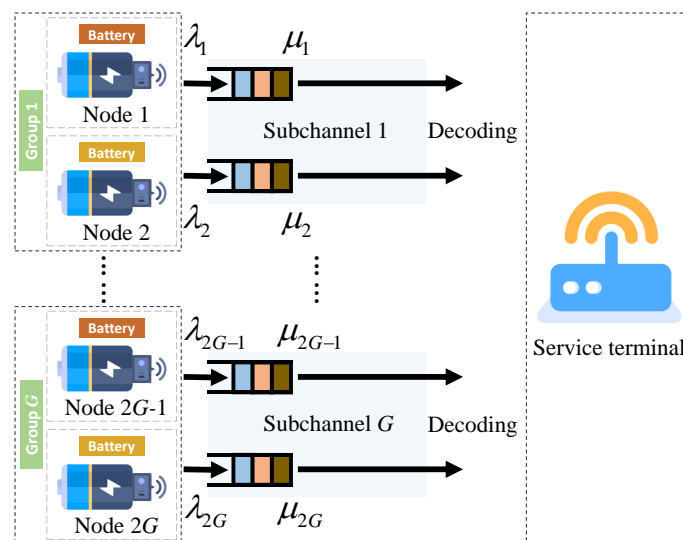


Figure 1. System model.

2.1. Channel Estimation

Sub-channel 1 is a Rayleigh-fading channel [29] that follows the independent distribution. We use α_i to represent the path loss coefficient of node i , and $h_i(n)$ to denote the Rayleigh-fading channel coefficient of the i -th node, which follows a complex Gaussian distribution. We denote $f_i(n) = |h_i(n)|^2$, which indicates that the channel gain of node i is a random variable with an index with a mean of $1/k_i$ and $1/k_i^2$. The distribution function of $f_i(n)$ is $k_i \exp(-k_i|h_i|^2)$. The sensor node transmits an independent signal with the transmission power P_i , where $B_i(n)$ represents the transmission signal of the node i and d_i represents the distance from the sensor node to the service terminal. $n_0(n)$ is an additive Gaussian white noise (AWGN) with mean value N_0 . The additive signal, $C(n)$, received by the service terminal in the time slot, n , is as follows:

$$C(n) = h_1(n)B_1(n) + h_2(n)B_2(n) + n_0(n) \tag{1}$$

The serving terminal can only serve information from the sensor node, i , if the received signal interference plus noise ratio (SINR) is greater than the threshold value v_i . If the serving terminal successfully receives the message from the sensor node, an ACK frame is sent. If the service is not finished, a NACK frame is sent, and the message is held at the head

of the queue until being retransmitted in a time slot. It is expected that the control channel sends ACK and NACK packets with no errors or delays. The sensor nodes and service terminal are considered to be fully aware of the channel status information (CSI) [30].

2.2. Data Queue Model

The data packet arrival process from the sensor node is an independent Bernoulli process, and each packet is fixed in size. The arrival rate of the update package respectively obeys the geometric distributions of λ_1 and λ_2 , respectively, so the probability of reaching a packet in the time slot, n , is as follows:

$$\Pr(N = n) = (1 - \lambda_i)^{n-1} \lambda_i \quad (2)$$

Each sensor node has a data queue Q_i that transmits to the service terminal. The data queue of the sensor node integrates with the process at the service terminal, which essentially consists of the queuing process awaiting the transmission of the data queue. We use the Geom/Geom/1 discrete-time queueing system to simulate changes in the sensor node's data queue. We consider an early access (EA) system; the data packet arrives at the end of the time slot, and the departure of the data packet occurs before the time slot boundary. In addition, the service terminal's duration for the data packet is an integer multiple of the time slot. Each sensor node has an infinite buffer to hold the generated packet. All data packets accept the service in the form of first-in-first-out (FIFO), the service time is S_i , and the service rate μ_i is the probability of successful transmission in the current time slot.

2.3. Decoding Scheme

To optimize the utilization of limited spectrum resources, sensor nodes transmit data to the service terminal using the same subchannel simultaneously. This concurrent transmission inevitably leads to interference among the sensor nodes. The data from a sensor node can be decoded by the service terminal only when the SINR surpasses a specific threshold. To address the varied interference environments, the service terminal employs three decoding strategies: interference decoding, traditional SIC decoding, and an improved SIC decoding strategy.

- Interference decoding (strategy A). In this strategy, the service terminal treats signals from two sensor nodes as mutual interference. To decode information from sensor node 1, it regards signals from sensor node 2 purely as interference, and vice versa. The service terminal attempts to decode the signals from each node amidst the cumulative interference and noise, treating the undesired signal as part of the background noise.
- Serial interference cancellation (strategy B). The service terminal employs a SIC strategy that first attempts to decode the information from one sensor node while considering the other's signal as interference. Upon successful decoding and removal of the first node's signal, it aims to decode the second node's information without interference. If the initial decoding fails, it would interfere with the subsequent decoding process, leading to potential failure in decoding the second node's information.
- Enhanced SIC strategy with error handling (strategy C). This approach is an enhanced SIC strategy. If the first node's message is decoded successfully, the terminal proceeds to decode sensor node 2's information as per the standard SIC procedure. Uniquely, if the decoding of sensor node 1 fails, the terminal still attempts to decode sensor node 2's signal. In this scenario, the service terminal continues to try to decode the signal from sensor node 2 by treating the signal from sensor node 1 as interference.

2.4. The Stability of the Queue

The stability of the system is a key performance indicator. The stability of the queue refers to the equilibrium between the data that enters and exits the queue. For an infinite length of time, the amount of time that newly arriving data wait in the queue to be served

does not grow indefinitely. Specifically, a data queue is considered stable if its length is finite. The formal definition of the stability of the queue is as follows:

Definition 1 (queue stability). Use Q_n^i to indicate the length of the time queue i (where $i \in \{0, 1, 2, \dots\}$) at the beginning of the discrete-time system n (where $n \in \{0, 1, 2, \dots\}$) starts; $\Pr\{\cdot\}$ represents the probability of a given event. If $\lim_{n \rightarrow \infty} \Pr\{Q_n^i < x\} = F(x)$ and $\lim_{x \rightarrow \infty} F(x) = 1$, the queue is stable.

Loynes' Law explains the relationship between arrival rates and service rates clearly [31]. If the queue remains steady, the average service rate of the service terminals must exceed the average packet arrival rate. If the opposite is not true, the queue length will grow infinitely, resulting in queue instability. The stable transmission area refers to the range of system-stable work in a wireless sensing network in a wireless sensing network. The stable transmission area consists of the arrival rate of a stable node of multiple queues. This article studies the stable transmission area with two nodes as an example, and the formal definition of the stable transmission area is as follows:

Definition 2 (stable transmission area). Use λ_1 to represent the arrival rate of node 1 data packet, and use λ_2 to represent the arrival rate of node 2 data packets. The stable transmission area, R , is defined as the two-node arrival rate collection; that is, $R = \{(\lambda_1, \lambda_2)\}$

2.5. Age of Information

AoI is a new metric used to measure the freshness of information. It indicates the time elapsed since the generation of successfully received packets. This metric is vital for applications that require frequent updates and timely decision-making. The more recent the information, the fresher it is.

AoI ΔN , in the discrete-time system, is defined as follows:

Definition 3 (age of information). At any time slot, n , the current time, n , and the service terminal receive the latest observed data packets to generate a difference between the times, $G(n)$, as follows:

$$\Delta N = n - G(n) \quad (3)$$

In discrete-time systems, the AoI remains constant at the current time slot. The AoI changes when the time slot changes.

3. Stable Transmission Region

We use stochastic dominance techniques [32] to deconstruct the interaction between two sensor data queues. Subsequently, we construct the dominant system to calculate the average service rate of service terminals to data queues.

Next, we evaluate the stable transmission regions of the three decoding strategies while considering the constraints of queue stability. We determine these stable transmission regions based on the arrival rate constraints necessary to achieve stable transmission. The stability constraints established in this section serve as the theoretical groundwork for the subsequent analysis of timeliness in the following section.

3.1. Strategy A (Interference Decoding) Stabilization Region

This decoding strategy is distinguished by the independence of decoding success or failure between sensor nodes. Subsequently, we compute the arrival rate constraints necessary for stabilizing two data queues under this decoding strategy. Let $D_{i/\varepsilon}$ denote the event that the data queue from sensor node i is successfully decoded by the service terminal when both sensor node 1 and sensor node 2 send packets, where $\varepsilon = 1, 2$. Similarly, let $D_{i/i}$ denote the event that the data queue from sensor node i is successfully decoded by

the service terminal when only sensor node i sends packets. The probability of an event occurring is denoted by $\Pr\{\cdot\}$. The average service rate $\mu_{1,A}$ of sensor node 1 and the average service rate $\mu_{2,A}$ of sensor node 2 under decoding strategy A can be represented as follows:

$$\mu_{1,A} = \Pr\{Q_2 = 0\} \times \Pr\{D_{1/1}\} + \Pr\{Q_2 > 0\} \times \Pr\{D_{2/1,2}\}, \tag{4}$$

$$\mu_{2,A} = \Pr\{Q_1 = 0\} \times \Pr\{D_{2/2}\} + \Pr\{Q_1 > 0\} \times \Pr\{D_{2/1,2}\}, \tag{5}$$

When only one queue is transmitted, the service terminal can successfully decode the data packet from sensor node i only when the SNR received by the service terminal is greater than the threshold v_i . Hence, the event probability that data from sensor node i can be successfully decoded when only sensor node i data are transmitted in a queue can be expressed as follows:

$$\begin{aligned} \Pr\{D_{i/i}\} &= \Pr\{\text{SNR}_i \geq v_i\} \\ &= \exp\left(-\frac{k_i N_0 v_i}{P_i d_i^{-\alpha}}\right) \end{aligned} \tag{6}$$

When data queues from two sensor nodes are transmitted simultaneously, the data packets from the service terminal can be successfully decoded only if the SINR received at the service terminal is greater than the threshold v_i . The SINR signifies that while decoding the current queue, another queue and noise concurrently interfere with the decoding process of the current queue. When two nodes are simultaneously transmitting data, the information from node 2 is considered interference when decoding node 1. In this case, the SINR of node 1 is given by the following:

$$\text{SINR}_1 = \frac{|h_1|^2 P_1 d_1^{-\alpha}}{N_0 + |h_2|^2 P_2 d_2^{-\alpha}} \tag{7}$$

When two sensor nodes engage in simultaneous data transmission, the probability of successfully decoding the data queue of the first node can be expressed as $\Pr\{D_{1/1,2}\}$:

$$\begin{aligned} \Pr\{D_{1/1,2}\} &= \Pr\{\text{SINR}_1 > v_1\} \\ &= \frac{k_2 P_1 d_1^{-\alpha}}{P_2 d_2^{-\alpha} k_1 v_1 + k_2 P_1 d_1^{-\alpha}} \exp\left(-\frac{k_1 N_0 v_1}{P_1 d_1^{-\alpha}}\right) \end{aligned} \tag{8}$$

Similarly, when two nodes are simultaneously engaged in data transmission, the information from node 1 is regarded as interference when decoding node 2. The SINR of node 2 is represented as follows:

$$\text{SINR}_2 = \frac{|h_2|^2 P_2 d_2^{-\alpha}}{N_0 + |h_1|^2 P_1 d_1^{-\alpha}} \tag{9}$$

The event probability that the second data queue can be successfully decoded when data are transmitted from two sensor nodes can be expressed as follows:

$$\Pr\{D_{2/1,2}\} = \frac{k_1 P_2 d_2^{-\alpha}}{P_1 d_1^{-\alpha} k_2 v_2 + k_1 P_2 d_2^{-\alpha}} \exp\left(-\frac{k_2 N_0 v_2}{P_2 d_2^{-\alpha}}\right) \tag{10}$$

Then, Equations (4) and (5) can be written as follows:

$$\mu_{1,A} = \Pr\{Q_2 = 0\} \times \Pr\left\{\frac{|h_1|^2 P_1 d_1^{-\alpha}}{N_0} \geq v_1\right\} + \Pr\{Q_2 > 0\} \times \Pr\left\{\frac{|h_1|^2 P_1 d_1^{-\alpha}}{N_0 + |h_2|^2 P_2 d_2^{-\alpha}} \geq v_1\right\} \quad (11)$$

$$\mu_{2,A} = \Pr\{Q_1 = 0\} \times \Pr\left\{\frac{|h_2|^2 P_2 d_2^{-\alpha}}{N_0} \geq v_2\right\} + \Pr\{Q_1 > 0\} \times \Pr\left\{\frac{|h_2|^2 P_2 d_2^{-\alpha}}{N_0 + |h_1|^2 P_1 d_1^{-\alpha}} \geq v_2\right\} \quad (12)$$

The first term in Equations (11) and (12) signifies that when another sensor node does not send packets, the average service rate of the service terminal to the current node depends only on the successful decoding probability of the current node under noise interference. The second term shows that when both sensor nodes have packets to send, one sensor’s sending operation interferes with the other’s decoding. The reason for this is that the service terminal must decode the data queue of another sensor while dealing with the interference caused by the data queue and noise of one of the nodes. The sending processes of both sensor nodes interact with each other, making it impossible to obtain an accurate average service rate. The construction of dominant systems can lead to breakdowns in their interactions. Next, we will consider the dominant system that is dominated by each sensor node separately.

We consider the first dominant system, which is dominated by the data queue of sensor node 1. In this system, when sensor node 1 does not have any data to transmit, it is assumed that it still sends virtual packets to the service terminal. The transmission of virtual packets from node 1 interferes with the decoding process at node 2. The process of transferring the data queue from sensor node 2 to the first master system is identical to that of the original system.

The following proposition gives the region of stable transmission for the first dominant system.

Proposition 1. *The stable transmission region of the first dominant system of strategy A is denoted by $R_{1,A}$ and given by Equation (13).*

$$R_{1,A} = \left\{ (\lambda_1, \lambda_2) : \left(1 - \frac{\lambda_2}{\frac{P_2 d_2^{-\alpha} k_1}{P_1 d_1^{-\alpha} k_2 v_2 + P_2 d_2^{-\alpha} k_1} \exp\left(-\frac{k_2 N_0 v_2}{P_2 d_2^{-\alpha}}\right)} \right) \frac{\exp\left(-\frac{k_1 N_0 v_1}{P_1 d_1^{-\alpha}}\right)}{\lambda_1} + \frac{\lambda_2}{\frac{P_2 d_2^{-\alpha} k_1}{P_1 d_1^{-\alpha} k_2 v_2 + P_2 d_2^{-\alpha} k_1} \exp\left(-\frac{k_2 N_0 v_2}{P_2 d_2^{-\alpha}}\right) \lambda_1} \frac{P_1 d_1^{-\alpha} k_2}{P_2 d_2^{-\alpha} k_1 v_1 + P_1 d_1^{-\alpha} k_2} \exp\left(-\frac{k_1 N_0 v_1}{P_1 d_1^{-\alpha}}\right) > 1, \right. \quad (13)$$

$$\left. \text{for } 0 \leq \lambda_2 \leq \frac{P_2 d_2^{-\alpha} k_1}{P_1 d_1^{-\alpha} k_2 v_2 + P_2 d_2^{-\alpha} k_1} \exp\left(-\frac{k_2 N_0 v_2}{P_2 d_2^{-\alpha}}\right), \lambda_1 \geq 0 \right\}$$

Proof. In the first dominant system, as sensor node 1 continuously sends virtual packets to the service terminal, the data queue of sensor node 1 is never emptied. Thus, the probability that $\Pr\{Q_1\} = 0$ is equal to 0 and $\Pr\{Q_1 > 0\} = 1$ is equal to 1. Remembering that the average service rate of the service terminal for data from the queue of sensor node 2 is $\hat{\mu}_{2,A}$, Equation (12) can be written as follows:

$$\hat{\mu}_{2,A} = \frac{P_2 d_2^{-\alpha} k_1}{P_1 d_1^{-\alpha} k_2 v_2 + P_2 d_2^{-\alpha} k_1} \exp\left(-\frac{k_2 N_0 v_2}{P_2 d_2^{-\alpha}}\right) \quad (14)$$

Loynes’ criteria define a stable data queue at sensor node 2 as one in which the average service rate exceeds the average arrival rate, i.e., $\lambda_2 < \hat{\mu}_{2,A}$. The status of the service terminal to sensor node 1’s data queue is determined by sensor node 2’s queue state.

Applying Little’s law [33], we can calculate the probability of continuous data transmission in the data queue of sensor node 2 as follows:

$$\Pr\{Q_2 > 0\} = \frac{\lambda_2}{\hat{\mu}_{2,A}}. \tag{15}$$

The average service rate of node 1 in the first dominant system is derived from Equation (11), as follows:

$$\hat{\mu}_{1,A} = \left(1 - \frac{\lambda_2}{\frac{P_2 d_2^{-\alpha} k_1}{P_1 d_1^{-\alpha} k_2 v_2 + P_2 d_2^{-\alpha} k_1} \exp\left(-\frac{k_2 N_0 v_2}{P_2 d_2^{-\alpha}}\right)} \right) \exp\left(-\frac{k_1 N_0 v_1}{P_1 d_1^{-\alpha}}\right) \tag{16}$$

The first dominant system is regarded as stable only if both queues are stable at the same time and the average packet service rate is greater than the average arrival rate, i.e., $\lambda_1 < \hat{\mu}_{1,A}$ and $\lambda_2 < \hat{\mu}_{2,A}$ hold simultaneously. Bringing Equations (16) and (14) into simplification yields a formula for the stable transmission region, $R_{1,A}$, of the first dominant system as in Equation (13).

See Appendix A.1. □

Next, we consider the second dominant system, which is dominated by the data queue of sensor node 2. In this system, even if sensor node 2 has no data to transmit, it sends virtual packets to the service terminal. The transmission procedure for sensor node 1 stays unaltered.

The stabilization region of the second dominant system is given by the following Proposition:

Proposition 2. *The stabilized transmission region of the second dominant system of scheme a is denoted by $R_{2,A}$ and is given by Equation (17).*

$$R_{2,A} = \left\{ (\lambda_1, \lambda_2) : \left(1 - \frac{\lambda_1}{\frac{P_1 d_1^{-\alpha} k_2}{P_2 d_2^{-\alpha} k_1 v_1 + P_1 d_1^{-\alpha} k_2} \exp\left(-\frac{k_1 N_0 v_1}{P_1 d_1^{-\alpha}}\right)} \right) \frac{\exp\left(-\frac{k_2 N_0 v_2}{P_2 d_2^{-\alpha}}\right)}{\lambda_2} + \frac{\lambda_1}{\frac{P_1 d_1^{-\alpha} k_2}{P_2 d_2^{-\alpha} k_1 v_1 + P_1 d_1^{-\alpha} k_2} \exp\left(-\frac{k_1 N_0 v_1}{P_1 d_1^{-\alpha}}\right) \lambda_2} \frac{P_2 d_2^{-\alpha} k_1}{P_1 d_1^{-\alpha} k_2 v_2 + P_2 d_2^{-\alpha} k_1} \exp\left(-\frac{k_2 N_0 v_2}{P_2 d_2^{-\alpha}}\right) > 1, \right. \tag{17}$$

$$\left. \text{for } 0 \leq \lambda_1 \leq \frac{P_1 d_1^{-\alpha} k_2}{P_2 d_2^{-\alpha} k_1 v_1 + P_1 d_1^{-\alpha} k_2} \exp\left(-\frac{k_1 N_0 v_1}{P_1 d_1^{-\alpha}}\right), \lambda_2 \geq 0 \right\}$$

Proof. The queue of sensor node 2 is never emptied; $\Pr\{Q_2 = 0\}$ is equal to 0 in Equation (11). In the second dominant system, the average service rate, $\hat{\mu}_{1,A}$, of the service terminal to the data queue of sensor node 1 is denoted as follows:

$$\hat{\mu}_{1,A} = \frac{P_1 d_1^{-\alpha} k_2}{P_2 d_2^{-\alpha} k_1 v_1 + P_1 d_1^{-\alpha} k_2} \exp\left(-\frac{k_1 N_0 v_1}{P_1 d_1^{-\alpha}}\right) \tag{18}$$

Using the Loynes criterion, the transmission process of sensor node 1’s data queue is deemed stable if the average service rate surpasses the average arrival rate; that is, $\lambda_1 < \hat{\mu}_{1,A}$. The service status of sensor node 2 at the time of the service terminal is determined by whether data are transferred from sensor node 1. Little’s law can be used to calculate the probability of data transmission in the data queue of sensor node 1 as follows:

$$\Pr\{Q_1 > 0\} = \frac{\lambda_1}{\hat{\mu}_{1,A}} \tag{19}$$

Equations (18) and (19) are brought into Equation (12) to derive the average service rate of sensor node 2 in the second dominant system:

$$\hat{\mu}_{2,A} = \left(1 - \frac{\lambda_1}{\frac{P_1 d_1^{-\alpha} k_2}{P_2 d_2^{-\alpha} k_1 v_1 + P_1 d_1^{-\alpha} k_2} \exp\left(-\frac{k_1 N_0 v_1}{P_1 d_1^{-\alpha}}\right)} \right) \exp\left(-\frac{k_2 N_0 v_2}{P_2 d_2^{-\alpha}}\right) \quad (20)$$

The second dominant system is regarded as stable only if both queues are stable at the same time and the average packet service rate is greater than the average arrival rate, i.e., $\lambda_1 < \hat{\mu}_{1,A}$ and $\lambda_2 < \hat{\mu}_{2,A}$ hold simultaneously. Simplifying this yields the stable transmission region $R_{2,A}$ of the second dominant system as in Equation (17). □

Proposition 3. *The stabilization region using the interference decoding strategy is denoted by R_A and is equal to the concatenation of the stabilization domains of the first dominant system and the second dominant system:*

$$R_A = R_{1,A} \cup R_{2,A}. \quad (21)$$

where $R_{1,A}$ and $R_{2,A}$ are given by Proposition 1—Equation (13) and Proposition 2—Equation (17), respectively.

Proof. The coupling between the queues of sensor nodes introduces complexity to the analysis process. To address this complexity, the stochastic dominance technique is introduced to decouple the interactions between queues. The stabilization region derived by this technique is both sufficient and necessary for the original system. This argument is thoroughly demonstrated in reference [32].

In summary, the stabilized transmission region consists of the concatenation of the stabilized regions of the first and second dominant systems. Therefore, we have Equation (21).

The derivation of some of the simplified formulas is presented in Appendix A. □

3.2. Strategy B (Serial Interference Cancellation) Stabilization Region

Strategy B uses serial interference cancellation, assuming that the channel conditions of the data queue of sensor node 1 are better than those of the data queue of sensor node 2. In this strategy, the service terminal first attempts to decode the data queue of sensor node 1. If it is successful, the interference from the data queue of sensor node 1 is removed from the synthesized signal, and the decoding of the data queue of sensor node 2 can continue. However, if the decoding of the data queue of sensor node 1 fails, the data queue of sensor node 2 cannot be decoded.

Denoting the average service rate of the service terminal using the SIC interference interruption strategy to the data queue of sensor node 1 by $\mu_{1,B}$, $\mu_{1,B}$ can be expressed as follows:

$$\mu_{1,B} = \Pr\{Q_2 = 0\} \times \Pr\{D_{1/1}\} + \Pr\{Q_2 > 0\} \times \Pr\{D_{2/1,2}\} \quad (22)$$

Using $\{D_{1/1,2}, D_{2/2}\}$ to denote the event where the data queue of sensor node 2 is successfully decoded following the successful decoding of the sensor node 1 data queue by the service terminal, the average service rate $\mu_{2,B}$ of the sensor node 2 data queue is denoted as follows:

$$\mu_{2,B} = \Pr\{Q_1 = 0\} \times \Pr\{D_{2/2}\} + \Pr\{Q_1 > 0\} \times \Pr\{D_{1/1,2}, D_{2/2}\} \quad (23)$$

If the data queues of two sensor nodes are transmitted simultaneously, the decoding process of the sensor node 2 data queue depends on the successful decoding of the sensor node 1 data queue. The interference-free decoding of sensor node 2 can be realized only after

the successful decoding of the sensor node 1 data queue. Therefore, $\{D_{1/1,2}, D_{2/2}\}$ can be derived as follows:

$$\begin{aligned} \Pr\{D_{1/1,2}, D_{2/2}\} &= \Pr\left\{\frac{|h_1|^2 P_1 d_1^{-\alpha}}{N_0 + |h_2|^2 P_2 d_2^{-\alpha}} \geq v_1, \frac{|h_2|^2 P_2 d_2^{-\alpha}}{N_0} \geq v_2\right\} \\ &= \frac{k_2 P_1 d_1^{-\alpha}}{k_2 P_1 d_1^{-\alpha} + P_2 d_2^{-\alpha} k_1 v_1} \exp\left[-\left(k_2 + \frac{P_2 d_2^{-\alpha} k_1 v_1}{P_1}\right) \cdot \frac{N_0 v_2}{P_2 d_2^{-\alpha}} - \frac{k_1 N_0 v_1}{P_1 d_1^{-\alpha}}\right] \end{aligned} \quad (24)$$

The service rate of the service terminal to the data queue of sensor node 2 is obtained as follows:

$$\begin{aligned} \mu_{2,B} &= \Pr\{Q_1 = 0\} \times \Pr\left\{\frac{|h_2|^2 P_2 d_2^{-\alpha}}{N_0} \geq v_2\right\} \\ &+ \Pr\{Q_1 > 0\} \times \Pr\left\{\frac{|h_1|^2 P_1 d_1^{-\alpha}}{N_0 + |h_2|^2 P_2 d_2^{-\alpha}} \geq v_1, \frac{|h_2|^2 P_2 d_2^{-\alpha}}{N_0} \geq v_2\right\} \end{aligned} \quad (25)$$

Since inter-queue interactions still exist, the stochastic dominance technique is still applied to obtain a stable transmission region.

For ease of presentation, $\Pr\left\{\frac{|h_1|^2 P_1 d_1^{-\alpha}}{N_0 + |h_2|^2 P_2 d_2^{-\alpha}} \geq v_1, \frac{|h_2|^2 P_2 d_2^{-\alpha}}{N_0} \geq v_2\right\}$ is denoted as m_1^B , $\Pr\left\{\frac{|h_1|^2 P_1 d_1^{-\alpha}}{N_0} \geq v_1\right\}$ is denoted as m_2^B , $\Pr\left\{\frac{|h_2|^2 P_2 d_2^{-\alpha}}{N_0 + |h_1|^2 P_1 d_1^{-\alpha}} \geq v_2\right\}$ is denoted as m_3^B , $\Pr\left\{\frac{|h_2|^2 P_2 d_2^{-\alpha}}{N_0} \geq v_2\right\}$ is denoted as m_4^B , and $\Pr\left\{\frac{|h_1|^2 P_1 d_1^{-\alpha}}{N_0 + |h_2|^2 P_2 d_2^{-\alpha}} \geq v_1\right\}$ is denoted as m_5^B .

In the first dominant system dominated by the data queue of sensor node 1, the following citations provide the stable transmission region of the first dominant system.

Proposition 4. *The stable transmission region of the first dominant system of strategy B is denoted by and given by Equation (26).*

$$R_{1,B} = \left\{(\lambda_1, \lambda_2) : \frac{\lambda_1}{m_2^B} + \frac{\lambda_1(m_2^B - m_3^B)}{m_2^B m_1^B} < 1, 0 \leq \lambda_2 \leq m_1^B, \lambda_1 \geq 0\right\} \quad (26)$$

Proof. In the first dominant system, $\Pr\{Q_1 > 0\} = 1$, the average service rate of the service terminal to the data queue of sensor node 2 is denoted by $\hat{\mu}_2^B$, i.e., $\hat{\mu}_{2,B} = m_1^B$. Using Little's theorem, the probability that the data queue of sensor node 2 is not empty is as follows:

$$\Pr\{Q_2 > 0\} = \frac{\lambda_2}{\hat{\mu}_{2,B}} \quad (27)$$

Bringing Equation (27) into Equation (22), according to Loynes' theorem, the first dominant system is stabilized when $\lambda_1 < \hat{\mu}_{1,B}$ and $\lambda_2 < \hat{\mu}_{2,B}$ hold simultaneously. The stabilized transmission region of the first dominant system under strategy B can be found in Equation (26)

See Appendix A.2. \square

In the second dominant system dominated by the data queue of sensor node 2, the stable transmission region is given by the following proposition:

Proposition 5. *The stabilized transmission region of the second dominant system of strategy B is denoted by $R_{2,B}$ and is presented in Equation (28).*

$$R_{2,B} = \left\{(\lambda_1, \lambda_2) : \frac{\lambda_1(m_4^B - m_1^B)}{m_5^B m_4^B} + \frac{\lambda_2}{m_4^B} < 1, \text{ for } 0 \leq \lambda_1 \leq m_5^B, \lambda_2 \geq 0\right\} \quad (28)$$

Proof. In the second dominant system, we can obtain $\Pr\{Q_2 > 0\} = 1$. The average service rate of the service terminal to the data queue of sensor node 1 is denoted by $\hat{\mu}_{1,B}$, i.e., $\mu_{1,B} = m_3^B$.

Using Little’s theorem, the probability that the data queue of sensor node 1 is non-empty is as follows:

$$\Pr\{Q_1 > 0\} = \frac{\lambda_1}{\hat{\mu}_{1,B}} \tag{29}$$

Bringing Equation (29) into Equation (23), the queue is stable when the constraints of Loynes’ theorem are satisfied, i.e., $\lambda_1 < \hat{\mu}_{1,B}$ and $\lambda_2 < \hat{\mu}_{2,B}$ hold simultaneously. We can obtain the stable transmission region of the second dominant system under strategy B, given by Equation (28). □

Proposition 6. *The stabilization region of the decoding strategy using SIC is denoted by R_B , i.e., $R_B = R_{1,B} \cup R_{2,B}$, where $R_{1,B}$ and $R_{2,B}$ are given by Equations (26) and (28).*

Proof. This proof follows a similar approach to that of Proposition 3 and involves utilizing stochastic dominance techniques to derive stable transmission regions. Due to its similarity, the detailed derivation of some simplified formulas is provided in Appendix A. □

3.3. Strategy C (Enhanced SIC Strategy with Error Handling) Stabilization Region

Decoding strategy C, referred to as an enhanced SIC strategy with error handling, represents an improvement over strategy B by increasing the probability of successful decoding for the data queue of sensor node 2. In this approach, even if the service terminal fails to decode the data queue of sensor node 1, it proceeds to re-decode the data queue of sensor node 2 and treat the data queue of sensor node 1 as interference. This is different from strategy B, where the decoding of the data queue of sensor node 2 depends on the successful decoding of the data queue of sensor node 1. Therefore, strategy C increases the probability of successful decoding for sensor node 2’s data queue, contributing to improved overall system performance.

By $\mu_{1,C}$, we denote the average service rate of the service terminal using decoding policy C to the data queue of sensor node 1, as expressed in Equation (30):

$$\mu_{1,C} = \Pr\{Q_2 = 0\} \times \Pr\{D_{1/1}\} + \Pr\{Q_2 > 0\} \times \Pr\{D_{2/1,2}\} \tag{30}$$

We use $\Pr\{D_{1/1,2}, D_{2/2}\}$ to denote the successful re-decoding of node 2 when two sensor nodes are transmitted at the same time, provided that node 1 fails to decode. The average service rate of the service terminal for the data queue of sensor node 2 can be expressed as follows:

$$\mu_{2,C} = \Pr\{Q_1 = 0\} \times \Pr\{D_{2/2}\} + \Pr\{Q_1 > 0\} \times (\Pr\{D_{1/1,2}, D_{2/2}\} + \Pr\{\overline{D_{1/1,2}}, D_{2/1,2}\}) \tag{31}$$

We decouple the interaction queue using the stochastic dominance technique. For ease of notation, $\Pr\left\{\frac{|h_1|^2 P_1 d_1^{-\alpha}}{N_0} \geq v_1\right\}$ is denoted as m_1^C , $\Pr\left\{\frac{|h_2|^2 P_2 d_2^{-\alpha}}{N_0} \geq v_2\right\}$ is denoted as m_2^C , $\Pr\left\{\frac{|h_1|^2 P_1 d_1^{-\alpha}}{N_0 + |h_2|^2 P_2 d_2^{-\alpha}} \geq v_1\right\}$ is denoted as m_3^C , $\Pr\left\{\frac{|h_1|^2 P_1 d_1^{-\alpha}}{N_0 + |h_2|^2 P_2 d_2^{-\alpha}} \geq v_1, \frac{|h_2|^2 P_2 d_2^{-\alpha}}{N_0 + |h_1|^2 P_1 d_1^{-\alpha}} \geq v_2\right\}$ is denoted as m_4^C , and $\left\{\frac{|h_1|^2 P_1 d_1^{-\alpha}}{N_0 + |h_2|^2 P_2 d_2^{-\alpha}} < v_1, \frac{|h_2|^2 P_2 d_2^{-\alpha}}{N_0 + |h_1|^2 P_1 d_1^{-\alpha}} \geq v_2\right\}$ is denoted as m_5^C .

In the first dominant system dominated by the data queue of sensor node 1, the following citations give the stable transmission region of the first dominant system.

Proposition 7. The stable transmission region of the first dominant system of strategy C is denoted by $R_{1,C}$ and is given by Equation (32).

$$R_{1,C} = \left\{ (\lambda_1, \lambda_2) : \frac{\lambda_1}{m_1^C} + \frac{\lambda_1(m_1^C - m_3^C)}{m_1^C(m_4^C + m_5^C)} < 1, \text{ for } 0 \leq \lambda_2 \leq m_4^C + m_5^C, \lambda_1 \geq 0 \right\} \quad (32)$$

Proof. In the first dominant system, which is governed by the data queue of sensor node 1, the average service rate of the service terminal to the data queue of sensor node 2 is denoted as $\hat{\mu}_{2,C}$. Specifically, $\hat{\mu}_{2,C} = m_4^C + m_5^C$.

Using Little's theorem, the probability that the data queue of sensor node 2 is non-empty is $\Pr\{Q_2 > 0\} = \frac{\lambda_1}{\hat{\mu}_{2,C}}$.

According to Loynes' theorem, i.e., $\lambda_1 < \hat{\mu}_{1,C}$ and $\lambda_2 < \hat{\mu}_{2,C}$ hold simultaneously, and the stable transmission region is presented in Equation (32).

See Appendix A.3. \square

In the second dominant system, which is dominated by the data queue of sensor node 2, the stable transmission region is defined by the following proposition:

Proposition 8. The stable transmission region of the second dominant system of strategy C is denoted by $R_{2,C}$ and is given by Equation (33).

$$R_{2,C} = \left\{ (\lambda_1, \lambda_2) : \frac{\lambda_1(m_2^C - m_4^C - m_5^C)}{m_3^C m_2^C} + \frac{\lambda_2}{m_2^C} < 1, \text{ for } 0 \leq \lambda_1 \leq m_3^B, \lambda_2 \geq 0 \right\} \quad (33)$$

Proof. In the second dominant system, where the data queue of sensor node 2 is dominant, the average service rate of the service terminal to the data queue of sensor node 1 is denoted as $\hat{\mu}_{1,C}$, and we have $\hat{\mu}_{1,C} = \Pr\{D_{2/1,2}\}$.

We employ Little's theorem and Loynes' criterion, which state that the system is stable when $\lambda_1 < \hat{\mu}_{1,C}$ and $\lambda_2 < \hat{\mu}_{2,C}$ hold simultaneously. The stable transmission region of the second dominant system is given by Equation (33). \square

Proposition 9. The stabilization region of the service terminal using the SIC interference interruption strategy is denoted by R_C , i.e., $R_C = R_{1,C} \cup R_{2,C}$, where $R_{1,C}$ and $R_{2,C}$ are given by Equations (32) and (33).

Proof. This proof is similar to that of Theorem 1 and is, therefore, omitted. The derivation of some of the simplified formulas is presented in Appendix A. \square

3.4. Discussion of the Stable Transmission Region

In order to better understand the stable transmission region, we provide some discussion of the stable transmission region. A schematic diagram of the stable transmission region of the OFDMA uplink system using the three policies to serve the terminals is shown in Figure 2, where the polygons O-A-B-C, O-A-D-C, and O-A-E-C denote the stable transmission regions R_A , R_B , and R_C , respectively, which are made up of the nodes' arrival rates.

Strategy A does not account for decoding failures and treats the messages from other users directly as interference. Strategy A is not affected by the decoding success or failure of another user during the decoding process, so it stabilizes the transmission region to a minimum. Strategy B ignores the case of the decoding failure of user 1, so when user 1 fails to decode, it cannot decode user 2. Strategy C considers the case where user 1's decoding fails. Thanks to the attempt to recover user 2's message even after user 1's decoding failure, strategy C can obtain a larger stable transmission region than strategy B, i.e., $R_b \subset R_c$ always holds.

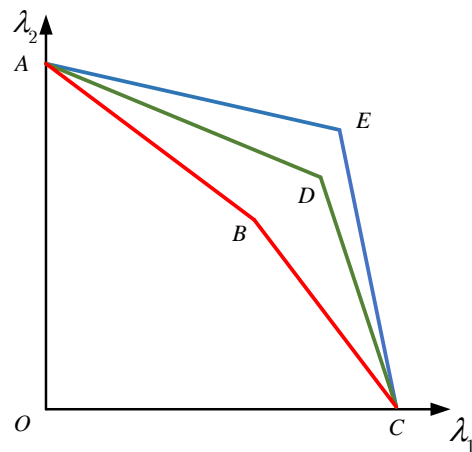


Figure 2. Stabilization regions corresponding to the three decoding strategies.

4. AoI Analysis

In this section, we investigate the network performance using the AoI as a metric when considering queue stability constraints. We propose a stable iterative algorithm to assess the minimum AoI of the system. Subsequently, we determine the minimum AoI for each decoding strategy and optimize the overall AoI of the system in a scenario with fixed transmit power to determine the most effective transmission strategy.

First, we conduct an initial analysis of the queueing model. For the data queue transmitted from each sensor node to the service terminal, the packet arrival process follows an independent Bernoulli process with an arrival rate of λ . The packet arrival rate is identical to the service process arrival rate. In each time slot, the service process can also be considered an independent Bernoulli process. According to the Bernoulli arrival process, the time slot interval between two consecutive arrivals has a geometric distribution. Therefore, each queuing system is equivalent to a Geom/Geom/1 queue, representing the queuing process as an early arrival system.

The average message age of a single queue is given by the following proposition:

Proposition 10. For a single packet with arrival rate λ , the average message age of a Geom/Geom/1 queue with service rate μ is $\overline{\Delta N}$:

$$\overline{\Delta N} = \frac{\lambda^2(1 - \mu)}{\mu^2(\mu - \lambda)} + \frac{1}{\mu} + \frac{1}{\lambda} \tag{34}$$

Proof. Figure 3 depicts the evolution of the AoI sample path of a data queue at a single node in a discrete-time system. The illustration shows that the m th data packet arrives at moment n_m and completes service, departing at moment n_m . The time interval between the arrival of the m th packet and the $(m - 1)$ th packet is denoted by X_m . W_m represents the waiting time for the m th packet to be served by the terminal after arriving at the queue, while S_m denotes the service time for the m th packet. The system time T_m indicates the duration that the m th packet remains in the system, expressed either as the sum of the waiting time W_m (which is a non-negative value) and the service time S_m (i.e., $T_m = W_m + S_m$), or as the sum of the arrival interval X_{m+1} of the $(m + 1)$ th packet and the waiting time W_{m+1} (i.e., $T_m = X_{m+1} + W_{m+1}$). It is evident that the system time T_{m-1} of the $(m - 1)$ th packet solely depends on the arrival interval and service time of the packet preceding the m th packet, independent of the arrival interval X_m of the m th packet. Therefore, given that the transmission system is in a steady state, the randomness of the system time for each packet remains consistent. The discrete-time AoI increases linearly within the time slot, and upon the service terminal’s observation of the latest packet arrival, the AoI resets to reflect the time the newest packet has spent waiting for service in the queue.

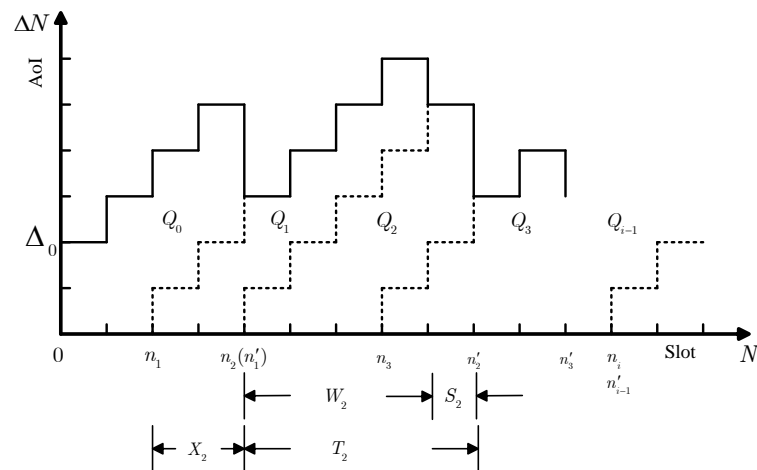


Figure 3. Discrete-time age of information sample paths.

To derive the discrete-time AoI, we decompose the graph as shown in Figure 3. The period between the m th packet and the $m + 1$ st packet, denoted as the period block ΔN_m , represents the AoI of the m th packet. The area of the period block signifies the AoI of the m th packet. The region under can be seen as the sum of region Q_0, Q_1, \dots and the triangular region Q_m with width T_m . Hence, we have the average discrete message age over the time interval of N , assuming that the service terminal receives a total of M packets, where $M = \max\{m | n_m \leq N\}$.

$$\begin{aligned} \overline{\Delta N} &= \lim_{N \rightarrow \infty} \frac{1}{N} \sum_{m=1}^M \Delta N_m \\ &= \lim_{N \rightarrow \infty} \frac{1}{N} (Q_0) + \lim_{N \rightarrow \infty} \frac{1}{N} \sum_{m=1}^{M-1} Q_m + \lim_{N \rightarrow \infty} \frac{1}{N} (Q_m) \end{aligned} \tag{35}$$

The triangular region Q_m in Equation (35) can be derived by solving the following:

$$\begin{aligned} Q_m &= \frac{1}{2} (T_{m-1} + X_m) (T_{m-1} + X_m + 1) - \frac{1}{2} (T_{m-1} + 1) T_{m-1} \\ &= T_{m-1} X_m + \frac{1}{2} X_m^2 + \frac{1}{2} X_m \end{aligned} \tag{36}$$

When $N \rightarrow \infty$, the values of the first and last terms of Equation (35) converge to 0, which can be obtained as follows:

$$\begin{aligned} \overline{\Delta N} &= \lim_{N \rightarrow \infty} \frac{m-1}{N} \frac{1}{m-1} \sum_{m=1}^{m-1} Q_m \\ &= \rho E[Q_m] \\ &= \rho \left(E[T_m X_m] + \frac{1}{2} E[X_m^2] + \frac{1}{2} E[X_m] \right) \end{aligned} \tag{37}$$

where ρ denotes the steady-state rate of the packet when the system is stabilized for steady transmission, i.e., $\rho = \lim_{N \rightarrow \infty} \frac{m-1}{N}$.

Under the Geom/Geom/1 queuing model, the packet arrival process and the service process are independent of each other at each time slot. Consequently, the service duration S_m and the packet arrival interval X_m are independently and identically distributed. Both S_m and X_m follow the geometric distribution, with the packet arrival rate denoted by λ and the service rate denoted by μ . The expected values of the arrival interval and the service duration are given by $E(X_m) = \frac{1}{\lambda}$ and $E(S_m) = \frac{1}{\mu}$.

Since the service duration S_m and the arrival interval X_m are independent, we have the following:

$$\begin{aligned} E[T_m X_m] &= E[(W_m + S_m)X_m] \\ &= E(W_m X_m) + E(S_m)E(X_m) \\ &= \frac{1 - \mu}{\mu - \lambda} \cdot \frac{\lambda}{\mu^2} + \frac{1}{\mu\lambda} \end{aligned} \tag{38}$$

See Appendix A.4.

According to the equation, $\rho = \lim_{N \rightarrow \infty} \frac{m-1}{N}$, as all the derivations of the previous term are conducted under a steady-state system, the steady-state rate ρ must exist and can be expressed in terms of the following expectations:

$$\rho = \frac{1}{E(X_m)} = \lambda \tag{39}$$

The results of Equations (38) and (39) are substituted into Equation (37) to express the average AoI of the data queue at a single sensor node under the steady-state system:

$$\begin{aligned} \overline{\Delta N} &= \lambda E(Q_m) \\ &= \lambda \left(\frac{\lambda(1 - \lambda)}{\mu - \lambda} + \frac{1}{\mu\lambda} + \frac{1}{\lambda^2} \right) \\ &= \frac{\lambda^2(1 - \lambda)}{\mu^2(\mu - \lambda)} + \frac{1}{\mu} + \frac{1}{\lambda} \end{aligned} \tag{40}$$

The AoI is expressed as a function of the packet arrival rate λ and the service rate μ , denoted as $\overline{\Delta N} = N(\lambda, \mu)$. □

Proposition 11. Denote the system average AoI of the sensor node i th data queue in the φ th dominant system as $[\bullet]^{(\varphi)}$, and when decoding strategy κ is used ($\kappa = A, B, C$), the uplink system average AoI $\overline{\Delta}_\kappa$ can be expressed as follows:

$$\overline{\Delta}_\kappa = \min \left\{ \left[\begin{aligned} &\frac{\lambda_1^2(1 - \hat{\mu}_1)}{\hat{\mu}_1^2(\hat{\mu}_1 - \lambda_1)} + \frac{1}{\hat{\mu}_1} + \frac{1}{\lambda_1} + \frac{\lambda_2^2(1 - \hat{\mu}_2)}{\hat{\mu}_2^2(\hat{\mu}_2 - \lambda_2)} + \frac{1}{\hat{\mu}_2} + \frac{1}{\lambda_2} \end{aligned} \right]^{(\varphi)} \mid \varphi = 1, 2 \right\} \tag{41}$$

$[\hat{\mu}_{1,\varphi,\kappa} = \hat{\mu}_{1,\varphi,\kappa}(\lambda_2), \hat{\mu}_{2,\varphi,\kappa} = \hat{\mu}_{2,\varphi,\kappa}(\lambda_1), (\lambda_1, \lambda_2) \in R_{\varphi,\kappa}]$

where $\hat{\mu}_{i,\varphi,\kappa}$ denotes the service rate of the node i th data queue in the φ th dominant system, and $R_{\varphi,\kappa}$ denotes the stabilization region of the φ th dominant system under decoding strategy κ .

Proof. We denote the arrival rate of the sensor node 1 data queue as λ_1 and the service rate as μ_1 , and the arrival rate of the sensor node 2 data queue as λ_2 and the service rate as μ_2 . The discrete-time averaged AoI $\overline{\Delta N}_1$ and $\overline{\Delta N}_2$ for sensor node 1's data queue and sensor node 2's data queue are denoted as follows:

$$\overline{\Delta N}_1 = \frac{\lambda_1^2(1 - \lambda_1)}{\mu_1^2(\mu_1 - \lambda_1)} + \frac{1}{\mu_1} + \frac{1}{\lambda_1} \tag{42}$$

$$\overline{\Delta N}_2 = \frac{\lambda_2^2(1 - \lambda_2)}{\mu_2^2(\mu_2 - \lambda_2)} + \frac{1}{\mu_2} + \frac{1}{\lambda_2} \tag{43}$$

Based on the analysis of the stable region in the previous section, it is evident that the data queue transmissions of the two sensor nodes interact with each other, making it impossible to obtain the exact functional expression of the service rate. Therefore, under each decoding strategy, we utilize the stochastic dominance technique to construct the

dominant system separately, aiming to obtain the precise functional expression between the service rate and the arrival rate. In the first dominant system dominated by the data queue of node 1, the service rate $\hat{\mu}_2$ of the service terminal for the data queue of node 2 remains constant. The service rate $\hat{\mu}_1$ of the service terminal for the data queue of node 1 can be expressed as a function of λ_2 , i.e., $\hat{\mu}_1 = \hat{\mu}_1(\lambda_2)$. In the second dominant system dominated by the data queue of node 2, the service rate $\hat{\mu}_1$ of the service terminal for the data queue of node 1 remains constant. The service rate of the service terminal for the data queue of node 2, $\hat{\mu}_2$, can be expressed as a function of λ_1 , i.e., $\hat{\mu}_2 = \hat{\mu}_2(\lambda_1)$. The AoI of the two nodes' data queues can be expressed as a function of the arrival rates λ_1 and λ_2 . Hence, we have $\overline{\Delta N_1} = N(\lambda_1, \hat{\mu}_1(\lambda_2))$ and $\overline{\Delta N_2} = N(\lambda_2, \hat{\mu}_2(\lambda_1))$.

It is crucial to acknowledge that the primary challenge in calculating the AoI lies in the interactions between the cohorts. The average AoI based on the dominant system characterizes the average AoI of the original system. Each set of rate pairs (λ_1, λ_2) in the stable region of the two dominant systems, as well as the functional equation of the service rate, is derived under the constraints of stable transmission. The concatenation of the stable regions of the two dominant systems characterizes the stable region of the original system. Therefore, each set of rate pairs (λ_1, λ_2) in the stabilization region of the two dominant systems is realizable in the original system and ensures the stability of the original system transmission.

Hence, the average AoI of the original system can be expressed in terms of the minimum AoI in the two dominant systems. The system average AoI of sensor node i 's data queue in the φ th dominant system is denoted as $\overline{\Delta^{(\varphi)}}$, as follows:

$$\overline{\Delta^{(\varphi)}} = \overline{\Delta N_1^{(\varphi)}} + \overline{\Delta N_2^{(\varphi)}} \quad (44)$$

Then, the system average AoI $\overline{\Delta}$ can be expressed as follows:

$$\overline{\Delta} = \min \left\{ \overline{\Delta^{(\varphi)}} \mid \varphi = 1, 2 \right\} \quad (45)$$

Based on the above analysis, it can be concluded that the average AoI of the uplink system using the κ decoding strategy, where $\kappa = A, B, C$, is given by Equation (41). \square

When the decoding strategy is determined and the transmit power P_i of sensor node i is fixed, a functional expression for the stabilization region can be obtained. The minimum average AoI of the uplink system then depends solely on the rate pair (λ_1, λ_2) . With three different decoding strategies, the minimum average AoI in the same transmission scenario can be determined. This offers insights into the selection of decoding strategies in various transmission scenarios.

Under different decoding strategies, solving the minimum average AoI involves finding the minimum value of the objective function subject to multiple constraints, namely the following:

$$\begin{aligned} & \min \overline{\Delta}_\kappa \\ & s.t. \{ \lambda_{1,\kappa}, \lambda_{2,\kappa} \} \subseteq R_{1,\kappa} \cup R_{2,\kappa}, \\ & \mu_{1,\kappa} = \mu_{1,\kappa}(\lambda_{2,\kappa}), \\ & \mu_{2,\kappa} = \mu_{2,\kappa}(\lambda_{1,\kappa}) \end{aligned} \quad (46)$$

To achieve the optimal average AoI, it is necessary to explore all rate pairs (λ_1, λ_2) in the stabilization region. Hence, a stabilized iterative algorithm is designed to obtain the optimal average AoI and transmission parameters. Algorithm 1 outlines this stabilized iterative algorithm for the average AoI uplink. In this algorithm, the objective function traverses all possible values of the arrival rate in the stabilized region in the two dominant systems. It selects the smallest AoI value in the two dominant systems to obtain the minimum average AoI of the system and outputs the pair of rates (λ_1, λ_2) that achieves the optimal average AoI.

Algorithm 1 Optimal information age based on the traversal algorithm.

Input: Packet arrival rate λ_i , packet service rate $\mu_1(\lambda_2), \mu_2(\lambda_1)$, first dominant system stability domain R_1 , second dominant system stability domain R_2 ;

Output: Minimize the average AoI $\overline{\Delta}_{\min}$, achieve the optimal average AoI for the rate pair (λ_1, λ_2) ;

- 1: In the first dominant system, λ_1 is initialized to 0; λ_2 is initialized to 0;
 - 2: **for** λ_1 to $\lambda_1^{\max} \in R_1$ **do**
 - 3: **for** λ_2 to $\lambda_2^{\max} \in R_1$ **do**
 - 4: The obtained rate pairs (λ_1, λ_2) are brought into the $\mu_1(\lambda_2), \mu_2(\lambda_1)$ equation;
 - 5: Bring in to solve for the average AoI $\overline{\Delta}^{(1)}$ of the first dominant system;
 - 6: λ_2 increase the step size;
 - 7: **end for**
 - 8: λ_1 increase the step size;
 - 9: **end for**
 - 10: Return the optimal average AoI $\overline{\Delta}^{(1)}$ of the first dominant system and the rate pair (λ_1, λ_2) that achieves the optimum;
 - 11: Follow the above steps to return the optimal average AoI $\overline{\Delta}^{(2)}$ in the second dominant system and realize the optimal rate pair (λ_1, λ_2) ;
 - 12: Compare the size of $\overline{\Delta}^{(1)}$ and $\overline{\Delta}^{(2)}$ and return the system optimal average AoI $\overline{\Delta}_{\min}$ and the corresponding rate pair (λ_1, λ_2) .
-

The iterative algorithm provided for stabilization is essentially the same as solving the fixed point issue. Algorithm 1 converges to a unique solution owing to the ergodicity of the adopted queueing model and the fixed-point theorem. Utilizing the aforementioned algorithm, we can obtain the optimal average AoI under different decoding strategies, along with the arrival rate parameter needed to achieve the optimal average AoI. By comparing the optimal average AoI of the three strategies, we can select the optimal transmission rate for the uplink system to balance stability and timeliness under the current transmission environment of the subchannels.

To verify the timeliness of the proposed hybrid OFDMA-NOMA system, we evaluate and compare its performance with that of the conventional OFDMA system. In an OFDMA system, two users alternate using a single resource block. When the data queue of the first user is non-empty, the second user remains silent and waits for transmission. Conversely, when the first user sends empty data, the second user gains permission to transmit. At this point, there is no further interaction between the queues. The probability that the i th user successfully sends is given by the following:

$$\Pr\{\text{SNR}_i^{\text{OFDMA}} \geq v_i\} = \exp\left(-\frac{k_i N_0 v_i}{P_i d_i^{-\alpha}}\right) \tag{47}$$

Therefore, the service rate of the service terminal for the two users can be expressed as follows: $\mu_1^{\text{OFDMA}} = \exp\left(-\frac{k_1 N_0 v_1}{P_1 d_1^{-\alpha}}\right)$ and $\mu_2^{\text{OFDMA}} = \left(1 - \lambda_1 \exp\left(-\frac{k_1 N_0 v_1}{P_1 d_1^{-\alpha}}\right)\right) \exp\left(-\frac{k_2 N_0 v_2}{P_2 d_2^{-\alpha}}\right)$, respectively. The system can stabilize transmission when the arrival rate is less than the service rate, i.e., $\lambda_i < \mu_i^{\text{OFDMA}}$. Under this constraint, the average AoI of the conventional OFDMA system is expressed as follows:

$$\begin{aligned} \overline{\Delta N} = & \frac{\lambda_1^2(1 - \lambda_1)}{(\mu_1^{\text{OFDMA}})^2(\mu_1^{\text{OFDMA}} - \lambda_1)} + \frac{1}{\mu_1^{\text{OFDMA}}} + \frac{1}{\lambda_1} \\ & + \frac{\lambda_2^2(1 - \lambda_2)}{(\mu_2^{\text{OFDMA}})^2(\mu_2^{\text{OFDMA}} - \lambda_2)} + \frac{1}{\mu_2^{\text{OFDMA}}} + \frac{1}{\lambda_2} \end{aligned} \tag{48}$$

5. Simulation Results

In this section, we provide numerical results and Monte Carlo simulations to evaluate the stabilized transmission area and AoI performance of the hybrid OFDMA-NOMA system. A total of 100 sensor nodes are considered, with the nodes divided into 50 groups, each containing 2 nodes. The groups are accessed using OFDMA technology, while the sensor nodes within the groups are accessed using NOMA technology. We consider the Rayleigh-fading channel, with path loss using the free-space path loss model. Unless there are other instructions, the parameter settings for each group are as follows, the Rayleigh-fading channel parameters are set to $k_1 = 2, k_2 = 5$, and the successful demodulation and decoding SNR thresholds are set to 0.3 dB. The path decay factor is $\alpha = 2$, and the distances between the two sensor nodes and the service terminal are 10 m and 15 m, respectively. In the simulation, we simulated 20 times and set the simulation time to 5000 slots.

Figure 4 depicts the stabilized region images of the three decoding strategies at a high decoding threshold ($v_i = 0.8$ dB), while Figure 5 illustrates the stabilized region images of the three decoding strategies at a low decoding threshold ($v_i = 0.2$ dB). The horizontal coordinate in the figure represents the arrival rate of the data queue of sensor node 1, while the vertical coordinate represents the arrival rate of the data queue of sensor node 2. The letters A, B, and C in the figure represent three distinct strategies of interference decoding, serial interference cancellation, and an enhanced SIC strategy with error handling, respectively.

Figure 4 illustrates that, when decoding thresholds are high, strategy A has the smallest stable transmission region, strategy B has a slightly larger stable transmission region than strategy A, and strategy C has the largest stable transmission region. Strategy A, which does not employ successive interference cancellation (SIC), must consider node 1 as interference when decoding node 2. This increases the difficulty of decoding node 2, which has poorer channel conditions, due to the better channel conditions of node 1. In contrast, the other two decoding strategies using SIC prioritize the decoding of node 1, which excludes the interference of node 1 from the total signal, thus increasing the decoding opportunity of node 2. Furthermore, strategy C, in comparison to strategy B, attempts to decode node 2 even in the event that node 1 fails to decode successfully. This approach, therefore, increases the probability of node 2 being successfully decoded, resulting in strategy C exhibiting the greatest degree of stability.

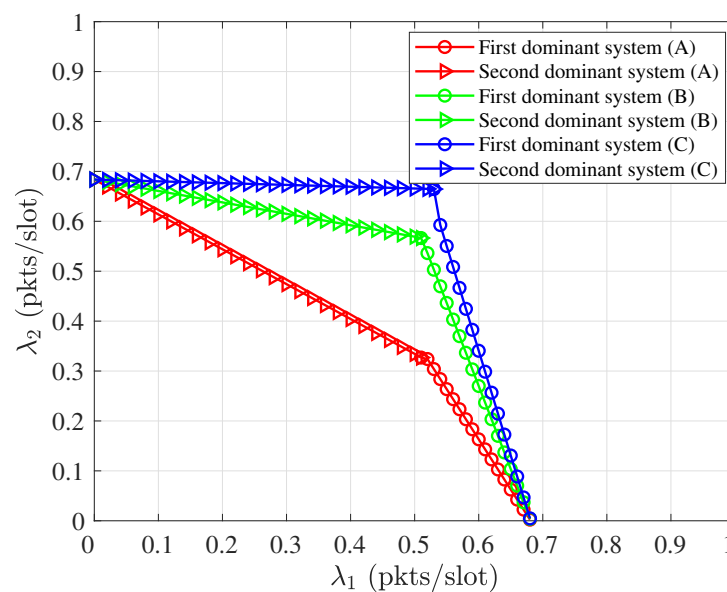


Figure 4. Stable regions of three decoding strategies at high decoding thresholds.

Figure 5 illustrates that the range comparison of the three decoding strategies for the low decoding threshold scenario is identical to that of the high decoding threshold scenario. Strategy C has the largest stable transmission region, followed by strategy B and strategy A. The probability of successful decoding for each node increases in the scenario with a low decoding threshold as compared to the scenario with a high decoding threshold. Consequently, each decoding strategy exhibits a more expansive range of stable regions at low decoding thresholds than at high decoding thresholds. It is important to note that a high arrival rate does not necessarily imply high timeliness, and the analysis of stable regions provides constraints for timeliness analysis.

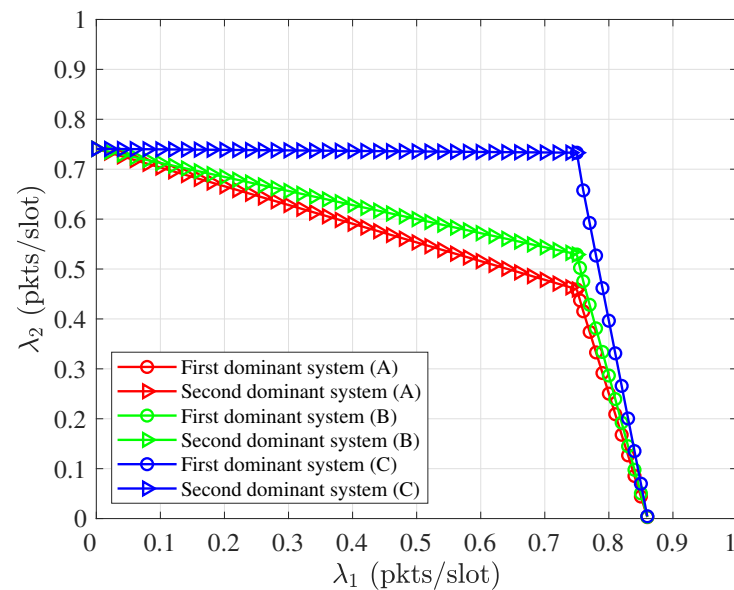


Figure 5. Stable regions of three decoding strategies at low decoding thresholds.

Set noise spectrum density to $N_0 = 4 \times 10^{-12}$. Figure 6 displays the image of the sensor data queue and average AoI when the lead system under the uplink wireless sensor network is used under the lead system with three decoding strategies. The x-axis represents the arrival rate of queue 1, the y-axis represents the arrival rate of queue 2, and the z-axis represents the system average AoI corresponding to the arrival rate.

The image of the average AoI shows a pattern of high values around its edges, with a concave shape in the center. Here, the minimum value at the concave indicates the optimal average AoI for the uplink. The figure corresponds to a higher AoI when the arrival rate is close to 0. When the update packet arrival rate of any node is close to 0, it means that almost no update packet arrives at that node, and the received information in the queue is stale, which reduces the freshness of the information, so the system has a larger value of AoI. This also corresponds to a higher AoI when the arrival rate of the update packet increases to the edge of the convergence region of stability and the packets are in the queue. The packets pile up in the queue and the newly arrived packets are not processed in time, reducing the freshness of the information. It is only when the arrival rate of each node reaches the value corresponding to the most concave point that the minimum AoI can be obtained, while the system is stable in transmission.

Figure 7 denotes the minimum AoI value of the system under the three decoding strategies statistically using a stable iterative algorithm with different transmit SNRs. The horizontal coordinate represents the transmit SNR and the vertical coordinate represents the minimum AoI of the system. The Monte Carlo simulation results agree very well with the analytical results. The AoI of the three decoding schemes shows a decreasing trend as the SNR increases. As the SNR increases, the decoding success rate increases, and the arriving packets can be served in time, so the AoI decreases.

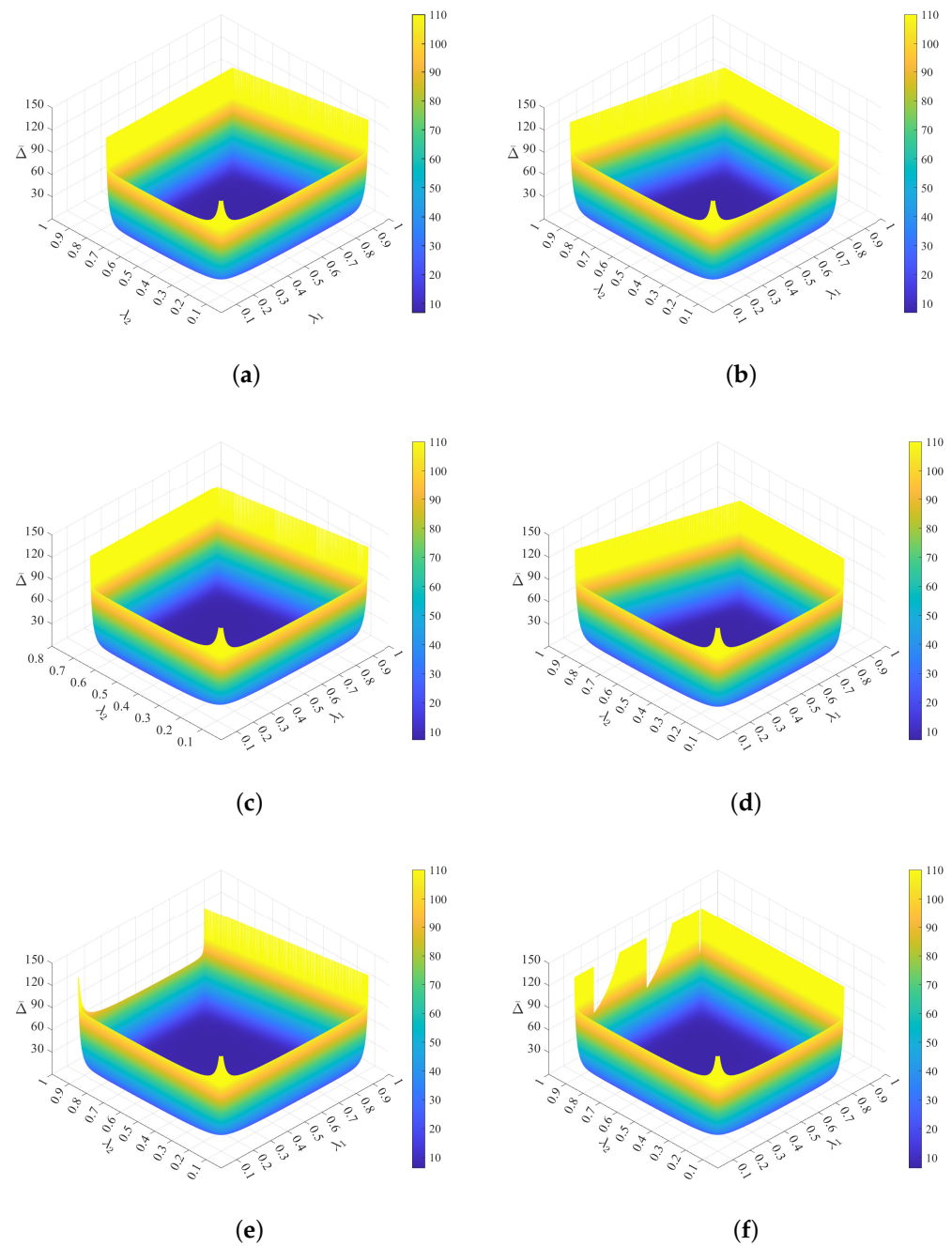


Figure 6. Age of information of the dominant system in the uplink. (a) Interference decoding: age of information for the first dominant system. (b) Interference decoding: age of information for the second dominant system. (c) Serial interference cancellation: age of information for the first dominant system. (d) Serial interference cancellation: age of information for the second dominant system. (e) Enhanced SIC strategy with error handling: age of information for the first dominant system. (f) Enhanced SIC strategy with error handling: age of information for the second dominant system.

Under the current channel parameter settings, as the SNR increases, the minimum average AoI of the three decoding strategies shows a gradually decreasing trend. When the SNR is low ($SNR = 5$ dB), the interference decoding strategy has a lower AoI, and the decoding method of mutually regarded interference, which directly regards the information from another node as interference, allows the update packet to be served in time even if it possesses a small stabilized area, thus resulting in a smaller average AoI. Under the current

channel parameters, the interference decoding strategy is used at a low SNR, which makes the system time-efficient and stable.

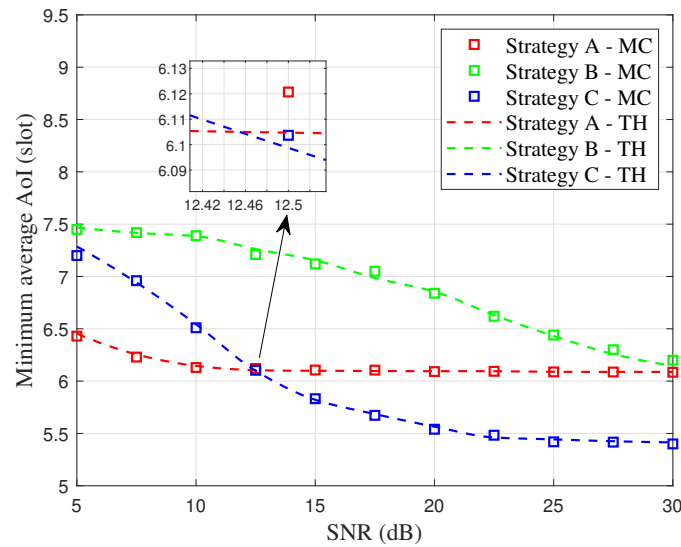


Figure 7. Minimum age of information for systems with different policies.

When the SNR is high ($SNR = 30$ dB), the enhanced SIC strategy with error handling is used to achieve a lower average AoI upper limit. Higher SNR levels increase interference from another data queue when using the interference decoding strategy, thus increasing the difficulty in decoding the queue. Using SIC, node 2 cannot decode after the failure of decoding the queue at node 1. The failure of decoding leads to untimely service and makes the information obsolete. Using an enhanced SIC strategy with error handling, the decoding success probability of node 2 is improved, the update packet obtains fast service with a smaller AoI, and the system is more time-sensitive while having stability.

The AoI comparison between the optimal policy of the hybrid OFDMA-NOMA system and the optimal policy of the conventional OFDMA system is shown in Figure 8. The Monte Carlo simulation results agree very well with the analytical results.

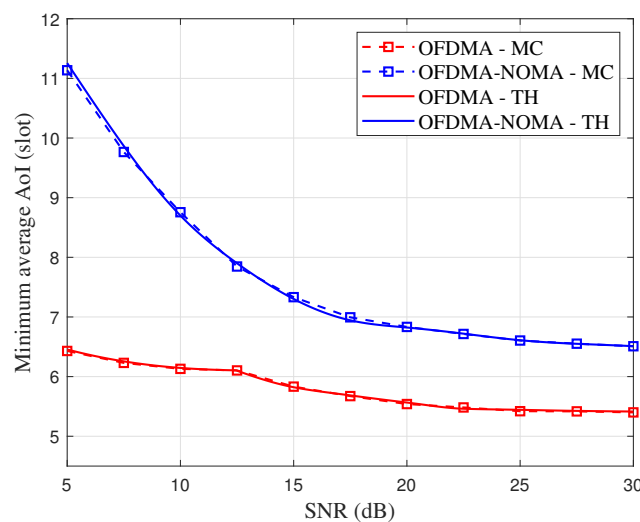


Figure 8. OFDMA-NOMA optimal policy vs. the OFDMA age of information.

The results show that our proposed hybrid OFDMA-NOMA outperforms the conventional OFDMA in terms of timeliness. When the SNR is low, our hybrid system has a greater advantage. When the SNR is low, node 2 in the conventional OFDMA system

has to wait until node 1's service is completed and the queue is empty before transmitting. In a low SNR environment, the probability of successfully decoding between two nodes decreases, leading to reduced transmission opportunities for node 2; this makes the information of node 2 stale, which makes the average AoI have a large value. When the SNR gradually increases, the average AoI of each scheme shows a decreasing trend, but our proposed optimal strategy is still better than the traditional scheme. When the SNR is large, the probability that both nodes can successfully decode increases, which leads to fast decoding for both nodes and reduces the value of AoI to some extent. However, the parallel transmission scheme still has an advantage over alternating transmissions. Figure 9 illustrates the average service rate corresponding to the optimal timeliness under stability constraints versus the signal-to-noise ratio. The simulation results align with the numerical analysis. Figure 9a demonstrates that the average service rate of node 1 gradually increases with the increase in the signal-to-noise ratio in the OFDMA system and the hybrid OFDMA-NOMA system. Moreover, the average service rate of node 1 in the OFDMA system is consistently higher than that in the hybrid OFDMA-NOMA system. Figure 9b illustrates that the average service rate of node 2 in the OFDMA system and hybrid OFDMA-NOMA system gradually increases with the increase in the signal-to-noise ratio. Furthermore, the average service rate of node 2 in the OFDMA system is consistently inferior to that of the hybrid OFDMA-NOMA system. As a consequence of the superior channel conditions of node 1, the service rate of node 1 is invariably greater than that of node 2 in the OFDMA system. This results in node 1 being consistently served, thereby reducing the service opportunity of node 2. In contrast, the optimal policy designed for the hybrid OFDMA-NOMA system effectively reduces the service rate of node 1 while enhancing the service rate of node 2. Furthermore, the parallel transmission of two nodes enhances the probability of node 2 being served. This approach allows both node 1 and node 2 to have the opportunity to be served, thereby reducing the average message age of the system.

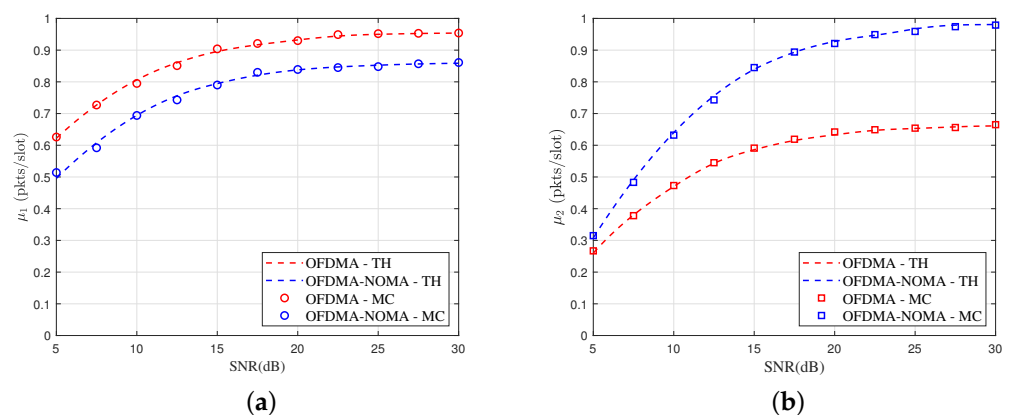


Figure 9. The relationship between the average service rate of node i and SNR. (a) The relationship between the average service rate of node 1 and SNR. (b) The relationship between the average service rate of node 2 and SNR.

6. Conclusions

In this paper, we study the stability and timeliness of OFDMA-NOMA systems, where each user has dynamic traffic arrivals. Within this system, two users form a group to share a resource block for simultaneous message transmissions. We consider three decoding schemes tailored to different transmission scenarios and employ the queueing theory to delineate the system's stable transmission region. We avoid the interplay between the two queues and obtain an explicit formula for the average AoI of the system. Furthermore, a stable iterative algorithm is used to calculate the minimum average AoI and find the optimal transmission strategy. Numerical validations underscore the superiority of the designed hybrid OFDMA-NOMA system over traditional OFDMA systems in enhancing timeliness while maintaining stability.

Author Contributions: Conceptualization, Y.D.; methodology, W.W. and Y.D.; writing—original draft preparation, W.W. and Y.D.; writing—review and editing, Y.D. and C.P.; revising the manuscripts. All authors have read and agreed to the published version of the manuscript.

Funding: The work of Y. Dong was supported by the National Natural Science Foundation of China (NSFC) under grant no. 62071237. The work of C. Pan was supported by the National Natural Science Foundation of China (NSFC) under grant no. 61931004.

Institutional Review Board Statement: Not applicable.

Informed Consent Statement: Not applicable.

Data Availability Statement: Data is contained within the article.

Acknowledgments: The authors would like to thank the editors and the reviewers for their insightful comments and suggestions, which resulted in substantial improvements to this work.

Conflicts of Interest: The authors declare no conflicts of interest.

Appendix A

Appendix A.1. Proof of Proposition 1

For the event probability that the data from a sensor node can be successfully decoded when only one sensor node's data queue is transmitted, we provide the following proof:

$$\begin{aligned}
 \Pr\{D_{i/i}\} &= \Pr\{\text{SNR}_i \geq v_i\} \\
 &= \Pr\left\{\frac{|h_i|^2 P_i d_i^{-\alpha}}{N_0} \geq v_i\right\} \\
 &= \Pr\left\{|h_i|^2 \geq \frac{N_0 v_i}{P_i d_i^{-\alpha}}\right\} \\
 &= \int_{\frac{N_0 v_i}{P_i d_i^{-\alpha}}}^{\infty} k_{i,D} \exp(-k_i |h_i|^2) d(|h_i|^2) \\
 &= \exp\left(-\frac{k_i N_0 v_i}{P_i d_i^{-\alpha}}\right)
 \end{aligned} \tag{A1}$$

For the event probability that the first data queue can successfully decode when two sensor nodes have data transmission at the same time, we provide the following proof:

$$\begin{aligned}
 \Pr\{D_{1/1,2}\} &= \Pr\{\text{SINR}_1 > v_1\} \\
 &= \Pr\left\{\frac{|h_1|^2 P_1 d_1^{-\alpha}}{N_0 + |h_2|^2 P_2 d_2^{-\alpha}} \geq v_1\right\} \\
 &= \Pr\left\{|h_1|^2 \geq \frac{N_0 + |h_2|^2 P_2 d_2^{-\alpha}}{P_1 d_1^{-\alpha}} v_1\right\} \\
 &= \int_0^{\infty} \int_{\frac{N_0 + |h_2|^2 P_2 d_2^{-\alpha}}{P_1 d_1^{-\alpha}} v_1}^{\infty} k_1 \exp(-k_1 |h_1|^2) k_2 \exp(-k_2 |h_2|^2) d(|h_1|^2) d(|h_2|^2) \\
 &= \int_0^{\infty} \exp\left(-\frac{N_0 + |h_2|^2 P_2 d_2^{-\alpha}}{P_1 d_1^{-\alpha}} k_1 v_1\right) k_2 \exp(-k_2 |h_2|^2) d(|h_2|^2) \\
 &= \frac{k_2 P_1 d_1^{-\alpha}}{P_2 d_2^{-\alpha} k_1 v_1 + k_2 P_1 d_1^{-\alpha}} \exp\left(-\frac{k_1 N_0 v_1}{P_1 d_1^{-\alpha}}\right)
 \end{aligned} \tag{A2}$$

Appendix A.2. Proof of Proposition 4

For the probability that the data queue of node 2 is successfully decoded when the service terminal successfully decodes the data queue of sensor node 1, we provide the following proof:

$$\begin{aligned}
\Pr\{D_{1/1,2}, D_{2/2}\} &= \Pr\left\{\frac{|h_1|^2 P_1 d_1^{-\alpha}}{N_0 + |h_2|^2 P_2 d_2^{-\alpha}} \geq v_1, \frac{|h_2|^2 P_2 d_2^{-\alpha}}{N_0} \geq v_2\right\} \\
&= \Pr\left\{|h_1|^2 \geq \frac{N_0 + |h_2|^2 P_2 d_2^{-\alpha}}{P_1 d_1^{-\alpha}} v_1, |h_2|^2 \geq \frac{N_0 v_2}{P_2 d_2^{-\alpha}}\right\} \\
&= \int_{\frac{N_0 v_2}{P_2 d_2^{-\alpha}}}^{\infty} \int_{\frac{N_0 + |h_2|^2 P_2 d_2^{-\alpha}}{P_1 d_1^{-\alpha}} v_1}^{\infty} k_1 \exp(-k_1 |h_1|^2) k_2 \exp(-k_2 |h_2|^2) d(|h_1|^2) d(|h_2|^2) \\
&= \frac{k_2 P_1 d_1^{-\alpha}}{k_2 P_1 d_1^{-\alpha} + P_2 d_2^{-\alpha} k_1 v_1} \exp\left[-\left(k_2 + \frac{P_2 d_2^{-\alpha} k_1 v_1}{P_1}\right) \cdot \frac{N_0 v_2}{P_2 d_2^{-\alpha}} - \frac{k_1 N_0 v_1}{P_1 d_1^{-\alpha}}\right] \quad (A3)
\end{aligned}$$

Appendix A.3. Proof of Proposition 7

When the data queues of two sensor nodes are transmitted at the same time, in the case where the decoding of the data queue of sensor node 1 fails, the data queue of node 1 is regarded as interference, and the event probability of the data queue of node 2 being successfully decoded is given as follows:

$$\begin{aligned}
\Pr\{\overline{D_{1/1,2}}, D_{2/1,2}\} &= \Pr\left\{\frac{|h_1|^2 P_1 d_1^{-\alpha}}{N_0 + |h_2|^2 P_2 d_2^{-\alpha}} < v_1, \frac{|h_2|^2 P_2 d_2^{-\alpha}}{N_0 + |h_1|^2 P_1 d_1^{-\alpha}} \geq v_2\right\} \\
&= \Pr\left\{|h_2|^2 > \frac{|h_1|^2 P_1 d_1^{-\alpha} - N_0 v_1}{P_2 d_2^{-\alpha} v_1}, |h_2|^2 \geq \frac{N_0 + |h_1|^2 P_1 d_1^{-\alpha}}{P_2 d_2^{-\alpha}} v_2\right\} \quad (A4)
\end{aligned}$$

It is easy to see that the continued solution of Equation (A4) requires a discussion on the case of magnitudes of $\frac{|h_1|^2 P_1 d_1^{-\alpha} - N_0 v_1}{P_2 d_2^{-\alpha} v_1}$ and $\frac{N_0 + |h_1|^2 P_1 d_1^{-\alpha}}{P_2 d_2^{-\alpha}} v_2$.

(1) if $\frac{|h_1|^2 P_1 d_1^{-\alpha} - N_0 v_1}{P_2 d_2^{-\alpha} v_1} \leq \frac{N_0 + |h_1|^2 P_1 d_1^{-\alpha}}{P_2 d_2^{-\alpha}} v_2$, we have $|h_1|^2 P_1 d_1^{-\alpha} (1 - v_1 v_2) \leq N_0 v_1 + N_0 v_1 v_2$.

The inequality holds if and only if $1 - v_1 v_2 \leq 0$, i.e., $v_1 v_2 \geq 1$.

Therefore, Equation (A4) can be derived as follows:

$$\begin{aligned}
\Pr\{\overline{D_{1/1,2}}, D_{2/1,2}\} &= \Pr\left\{|h_2|^2 > \frac{|h_1|^2 P_1 d_1^{-\alpha} - N_0 v_1}{P_2 d_2^{-\alpha} v_1}, |h_2|^2 \geq \frac{N_0 + |h_1|^2 P_1 d_1^{-\alpha}}{P_2 d_2^{-\alpha}} v_2\right\} \\
&= \Pr\left\{|h_2|^2 \geq \frac{N_0 + |h_1|^2 P_1 d_1^{-\alpha}}{P_2 d_2^{-\alpha}} v_2\right\} \\
&= \int_0^{\infty} \int_{\frac{N_0 + |h_1|^2 P_1 d_1^{-\alpha}}{P_2 d_2^{-\alpha}} v_2}^{\infty} k_1 \exp(-k_1 |h_1|^2) k_2 \exp(-k_2 |h_2|^2) d(|h_1|^2) d(|h_2|^2) \\
&= \frac{k_1 P_2 d_2^{-\alpha}}{P_1 d_1^{-\alpha} k_2 v_2 + k_1 P_2 d_2^{-\alpha}} \exp\left(-\frac{k_2 N_0 v_2}{P_2 d_2^{-\alpha}}\right) \quad (A5)
\end{aligned}$$

(2) If $1 - v_1 v_2 > 0$, we have $v_1 v_2 < 1$. For the integration limit, we have the following two possibilities: when $|h_1|^2 > \frac{N_0 v_1 + N_0 v_1 v_2}{P_1 d_1^{-\alpha} (1 - v_1 v_2)}$, then the integration limit of $|h_1|^2$ becomes

$\left(\frac{N_0v_1+N_0v_1v_2}{P_1d_1^{-\alpha}(1-v_1v_2)}, +\infty\right)$; if $|h_1|^2 < \frac{N_0v_1+N_0v_1v_2}{P_1d_1^{-\alpha}(1-v_1v_2)}$, then the integration limit of $|h_1|^2$ becomes $\left(0, \frac{N_0v_1+N_0v_1v_2}{P_1d_1^{-\alpha}(1-v_1v_2)}\right)$, so Equation (A4) can be written as follows:

$$\begin{aligned} \Pr\{\overline{D_{1/1,2}}, D_{2/1,2}\} &= \Pr\left\{|h_2|^2 > \frac{|h_1|^2P_1d_1^{-\alpha} - N_0v_1}{P_2d_2^{-\alpha}v_1}, |h_2|^2 \geq \frac{N_0 + |h_1|^2P_1d_1^{-\alpha}}{P_2d_2^{-\alpha}}v_2\right\} \\ &= \int_{\frac{N_0v_1+N_0v_1v_2}{P_1d_1^{-\alpha}(1-v_1v_2)}}^{+\infty} \int_{\frac{|h_1|^2P_1d_1^{-\alpha} - N_0v_1}{P_2d_2^{-\alpha}v_1}}^{+\infty} k_1 \exp(-k_1|h_1|^2) k_2 \exp(-k_2|h_2|^2) d(|h_1|^2) d(|h_2|^2) + \\ &\int_0^{\frac{N_0v_1+N_0v_1v_2}{P_1d_1^{-\alpha}(1-v_1v_2)}} \int_{\frac{N_0+|h_1|^2P_1d_1^{-\alpha}}{P_2d_2^{-\alpha}}v_2}^{+\infty} k_1 \exp(-k_1|h_1|^2) k_2 \exp(-k_2|h_2|^2) d(|h_1|^2) d(|h_2|^2) \\ &= \left\{1 - \exp\left[-\left(k_1 + \frac{P_1d_1^{-\alpha}k_2v_2}{P_2d_2^{-\alpha}}\right) \frac{N_0v_1 + N_0v_1v_2}{P_1d_1^{-\alpha}(1-v_1v_2)}\right]\right\} \\ &\times \frac{k_1P_2d_2^{-\alpha}}{P_1d_1^{-\alpha}k_2v_2 + k_1P_2d_2^{-\alpha}} \exp\left(-\frac{k_2N_0v_2}{P_2d_2^{-\alpha}}\right) \end{aligned} \tag{A6}$$

Appendix A.4. Proof of Proposition 10

For the joint expectation of arrival interval and waiting time, we provide the following proof:

Denote $\lambda_0 = (1 - \mu) / (1 - \lambda)$, and the probability density function of the system time T_m is as follows: $f_T(k) = (1 - \lambda_0)^{k-1} \lambda_0$. When given the $X_m = x$ condition, the conditional expectation of W_m is as follows:

$$\begin{aligned} E[W_m|X_m = x] &= E[(T_{m-1} - x)^+ | X_m = x] \\ &= E[(T - x)^+] \\ &= \sum_x^N (k - x) f_T(k) dk \\ &= \sum_x^N (k - x) (1 - \lambda_0)^{k-1} \lambda_0 dk \\ &= \frac{\lambda_0^x}{1 - \lambda_0} \end{aligned} \tag{A7}$$

We apply the expectation iteration to solve $E[W_m X_m]$:

$$\begin{aligned} E[W_m X_m] &= \sum_{x=1}^N x E[W_m | X_m = x] f_T(x) \\ &= \frac{\lambda}{\mu - \lambda} \frac{1 - \mu}{\mu^2} \\ &= \frac{1 - \mu}{\mu - \lambda} \cdot \frac{\lambda}{\mu^2} \end{aligned} \tag{A8}$$

References

- Zhao, Y.; Yu, G.; Xu, H. 6G mobile communication network: Vision, challenges and key technologies. *arXiv* **2019**, arXiv:1905.04983.
- You, G.; Zhu, Y. Structure and Key Technologies of Wireless Sensor Network. In Proceedings of the IEEE 2020 Cross Strait Radio Science & Wireless Technology Conference (CSRSWTC), Fuzhou, China, 13–16 December 2020; pp. 1–2.
- Li, L.; Dong, Y.; Pan, C.; Fan, P. Timeliness of wireless sensor networks with random multiple access. *J. Commun. Netw.* **2023**, *25*, 405–418. [[CrossRef](#)]
- Kaul, S.; Gruteser, M.; Rai, V.; Kenney, J. Minimizing age of information in vehicular networks. In Proceedings of the 2011 8th Annual IEEE Communications Society Conference on Sensor, Mesh and Ad Hoc Communications and Networks, Salt Lake City, UT, USA, 27–30 June 2011; pp. 350–358.

5. Semente, R.S.; Silva, A.; Salazar, A.O.; Oliveira, F.D.; Lock, A.S. A energy efficient WSN system for limited power source environments. In Proceedings of the IEEE 2013 Seventh International Conference on Sensing Technology (ICST), Wellington, New Zealand, 3–5 December 2013; pp. 193–197.
6. De Vries, J.P.; Simić, L.; Achtzehn, A.; Petrova, M.; Mähönen, P. The Wi-Fi “congestion crisis”: Regulatory criteria for assessing spectrum congestion claims. *Telecommun. Policy* **2014**, *38*, 838–850. [\[CrossRef\]](#)
7. Li, J.; Wu, X.; Laroia, R. *OFDMA Mobile Broadband Communications: A Systems Approach*; Cambridge University Press: Cambridge, UK, 2013.
8. Jamal, M.N.; Hassan, S.A.; Jayakody, D.N.K.; Rodrigues, J.J. Efficient nonorthogonal multiple access: Cooperative use of distributed space-time block coding. *IEEE Veh. Technol. Mag.* **2018**, *13*, 70–77. [\[CrossRef\]](#)
9. Shi, L.; Li, Z.; Bi, X.; Liao, L.; Xu, J. Full-duplex multi-hop wireless networks optimization with successive interference cancellation. *Sensors* **2018**, *18*, 4301. [\[CrossRef\]](#)
10. Shannon, C.E. A mathematical theory of communication. *Bell Syst. Tech. J.* **1948**, *27*, 379–423. [\[CrossRef\]](#)
11. Rong, B.; Ephremides, A. Cooperative access in wireless networks: Stable throughput and delay. *IEEE Trans. Inf. Theory* **2012**, *58*, 5890–5907. [\[CrossRef\]](#)
12. Palunčič, F.; Alfa, A.S.; Maharaj, B.T.; Tsimba, H.M. Queueing models for cognitive radio networks: A survey. *IEEE Access* **2018**, *6*, 50801–50823. [\[CrossRef\]](#)
13. Zhang, X.; Wang, F. Resource allocation for wireless power transmission over full-duplex OFDMA/NOMA mobile wireless networks. *IEEE J. Sel. Areas Commun.* **2018**, *37*, 327–344. [\[CrossRef\]](#)
14. Jeon, J.; Codreanu, M.; Latva-aho, M.; Ephremides, A. The stability property of cognitive radio systems with imperfect sensing. *IEEE J. Sel. Areas Commun.* **2013**, *32*, 628–640. [\[CrossRef\]](#)
15. Kompella, S.; Ephremides, A. Stable Throughput Regions in Wireless Networks. *Found. Trends® Netw.* **2014**, *7*, 235–338. [\[CrossRef\]](#)
16. Bouloukakakis, G.; Moscholios, I.; Georgantas, N.; Issarny, V. Performance analysis of internet of things interactions via simulation-based queueing models. *Future Internet* **2021**, *13*, 87. [\[CrossRef\]](#)
17. Dimitriou, I.; Pappas, N. Stable throughput and delay analysis of a random access network with queue-aware transmission. *IEEE Trans. Wirel. Commun.* **2018**, *17*, 3170–3184. [\[CrossRef\]](#)
18. Liu, X.; Xu, B.; Zheng, K.; Zheng, H. Throughput maximization of wireless-powered communication network with mobile access points. *IEEE Trans. Wirel. Commun.* **2023**, *22*, 4401–4415. [\[CrossRef\]](#)
19. Zheng, K.; Luo, R.; Wang, Z.; Liu, X.; Yao, Y. Short-term and long-term throughput maximization in mobile wireless-powered internet of things. *IEEE Internet Things J.* **2023**, *11*, 10575–10591. [\[CrossRef\]](#)
20. Zheng, K.; Liu, X.; Wang, B.; Zheng, H.; Chi, K.; Yao, Y. Throughput maximization of wireless-powered communication networks: An energy threshold approach. *IEEE Trans. Veh. Technol.* **2021**, *70*, 1292–1306. [\[CrossRef\]](#)
21. Liu, X.; Xu, B.; Wang, X.; Zheng, K.; Chi, K.; Tian, X. Impacts of sensing energy and data availability on throughput of energy harvesting cognitive radio networks. *IEEE Trans. Veh. Technol.* **2022**, *72*, 747–759. [\[CrossRef\]](#)
22. Kaul, S.; Yates, R.; Gruteser, M. Real-time status: How often should one update? In Proceedings of the 2012 Proceedings IEEE INFOCOM, Orlando, FL, USA, 25–30 March 2012; pp. 2731–2735.
23. Yates, R.D.; Kaul, S.K. The age of information: Real-time status updating by multiple sources. *IEEE Trans. Inf. Theory* **2018**, *65*, 1807–1827. [\[CrossRef\]](#)
24. Bedewy, A.M.; Sun, Y.; Shroff, N.B. Minimizing the age of information through queues. *IEEE Trans. Inf. Theory* **2019**, *65*, 5215–5232. [\[CrossRef\]](#)
25. Saurav, K.; Vaze, R. Online energy minimization under a peak age of information constraint. *IEEE J. Sel. Areas Inf. Theory* **2023**, *4*, 579–590. [\[CrossRef\]](#)
26. Zhang, S.; Wang, L.; Luo, H.; Ma, X.; Zhou, S. AoI-delay tradeoff in mobile edge caching with freshness-aware content refreshing. *IEEE Trans. Wirel. Commun.* **2021**, *20*, 5329–5342. [\[CrossRef\]](#)
27. Mohamed, A.G.; Gamal, M. Maximizing Stable Throughput in Age of Information-Based Cognitive Radio. In Proceedings of the 2022 IEEE International Conference and Expo on Real Time Communications at IIT (RTC), Chicago, IL, USA, 10–13 October 2022; pp. 1–7.
28. Maatouk, A.; Assaad, M.; Ephremides, A. Age-aware stochastic hybrid systems: Stability, solutions, and applications. *IEEE J. Sel. Areas Inf. Theory* **2023**, *4*, 762–783. [\[CrossRef\]](#)
29. Nguyen, T.N.; Tran, M.; Nguyen, T.L.; Ha, D.H.; Voznak, M. Multisource power splitting energy harvesting relaying network in half-duplex system over block Rayleigh fading channel: System performance analysis. *Electronics* **2019**, *8*, 67. [\[CrossRef\]](#)
30. Pappas, N.; Kountouris, M.; Ephremides, A.; Angelakis, V. Stable throughput region of the two-user broadcast channel. *IEEE Trans. Commun.* **2018**, *66*, 4611–4621. [\[CrossRef\]](#)
31. Loynes, R.M. The stability of a queue with non-independent inter-arrival and service times. In *Mathematical Proceedings of the Cambridge Philosophical Society*; Cambridge University Press: Cambridge, UK, 1962; Volume 58, pp. 497–520.
32. Rao, R.R.; Ephremides, A. On the stability of interacting queues in a multiple-access system. *IEEE Trans. Inf. Theory* **1988**, *34*, 918–930. [\[CrossRef\]](#)
33. Bertsekas, D.; Gallager, R. *Data Networks*; Athena Scientific: Nashua, NH, USA, 2021.

Disclaimer/Publisher’s Note: The statements, opinions and data contained in all publications are solely those of the individual author(s) and contributor(s) and not of MDPI and/or the editor(s). MDPI and/or the editor(s) disclaim responsibility for any injury to people or property resulting from any ideas, methods, instructions or products referred to in the content.